

## Chapter one

### 1-1 Introduction

The term focal liver lesion refers to circumscriptive and well-defined liver tumours, which can either be benign or malignant. The incidence of focal liver lesions has dramatically increased over the last few decades.(**Slocker JT, 2001**) This is mainly due to improved cross-sectional imaging techniques, which have increased the detection rate of focal liver lesions, especially as incidental findings on imaging initially performed for other abdominal or thoracic organs. Furthermore, the increase in cancer incidence worldwide has resulted in an increase in patients with metastatic liver disease, and also an increase in the incidence of patients with primary hepatic malignancies .(**Siegalr et al 2010 &Hattem et al 2006**).

The most common benign lesions are haemangioma (lesions consisting of a vascular proliferation), focal nodular hyperplasia (lesions consisting of a proliferation of bile ducts and well-functioning hepatocytes), adenoma (lesions consisting of a proliferation of poor functioning hepatocytes, with fat vacuoles, and the absence of bile ducts).( **Slocker 2001&Canon et al, 2010, and Gill et al,1983**) and cysts (fluid-filled cavities, probably arising from congenital defects in the development of bile ducts) . Malignant liver lesions can either consist of metastases from other malignancies like colorectal liver metastases (CRLM) and breast cancer metastases, or primary hepatic malignancies like hepatocellular carcinoma (HCC) and intrahepatic cholangiocellular carcinoma.

Treatment of these various types of focal liver lesions differs widely and may range from no treatment, follow-up, resection, radiofrequency ablation, chemotherapy or a combination thereof. In order to determine the optimal treatment strategy, adequate detection and characterization of focal liver lesions with non-invasive imaging techniques is utterly important. ( **Charlotte 2012**)

The real time imaging capabilities offered by widely available ultrasound (US) imaging modalities along with its inexpensive ,nonradioactive, and noninvasive natures makes it a first-line examination for screening of focal liver lesions (FLL). **(Jetendra et al 2013).**

However there are certain disadvantage associated with the use of conventional gray-scale us for characterization of focal liver lesions , there is limited sensitivity for detection of small focal liver lesions less than tow centimeter developed on cirrhotic liver which is already nodular or coarse-textured 3-5, Son graphic appearance of hepatocellular carcinoma (HCC) ,( primary malignant solid focal liver lesion) .and metastatic carcinoma (MET) ,(secondary malignant solid focal liver lesion) are highly overlapping **(Jetendra et al. 2013).**

The sensitivity of contrast –enhanced us ,contrast enhanced spiral computed tomography,and magnetic reasonance modalities for detection and characterization of focal liver lesions is higher than conventional gray-scale us ,but these modalities are not widely available, expensive and pose greate operational inconvenience. **(Jetendra et al. 2013).**

Although liver biopsy is gold standard for diagnosis of focal liver lesions but it is invasive and dangerous methods that can lead to spread of the tumor inside the human body. Therefore a computer-aided diagnostic (CAD) system for accurate characterization of primary and malignant liver lesions based on conventional gay-scaleus is highly desired to facilitate radiologist to clinical environment . **(Jetendra et al 2013)**

## **1-2 Problem of the study**

Liver lesions are considered seriously because of livers vital importance to human beings; characterization of liver lesions like hepatocellular carcinoma (HCC) and metastatic lesions(METS) using B-mode ultrasound it is a challenge for sonologist due to their highly dynamic range which lead to inconsistency of visual perception

characteristics, also other imaging modalities, computed tomography and magnetic resonance image also it got visual perception ramifications, the only proven method is the liver biopsy, is gold standard for diagnoses of liver lesions but it is invasive and hazardous methods, therefore a computer aided diagnostic system for accurate characterization for benign and malignant liver lesions based on conventional gray-scale ultrasound is highly desired, which might vote only the possible candidate for liver biopsy if needed.

### **1-3 Objectives**

#### **1-3-1 General objective**

To characterize benign and malignant liver lesions using ultrasonography and texture analysis, in order to have objective methods that can improve the accuracy of diagnosis and to reduce the number of invasive procedures

#### **1-3-2 Specific objectives**

- To develop a computer-aided diagnostic (CAD) system that differentiates between benign and malignant liver lesions in ultrasound image.
- To identify the distribution of the liver lesion in term of number, location, shape, size, and echo texture
- To classify the liver tissues into normal, benign and malignant using textural features.
- To find the accuracy of the applied algorithm and the classification power of the applied textural features and grey level
- To generate outline function that can identify liver lesions on U/S image in routine work
- To find the presence of the lesions vascularity using Doppler

#### **1-4 Significant of the study**

This study will give a reference that help in determination whether the liver lesion is benign, a primary malignant liver neoplasm or metastatic and also helps in limiting the using of liver biopsy to the highly suspected cases. As well as it will reduce the cost of the expensive other imaging modalities such as computed tomography, magnetic resonance image and contrast enhanced ultrasound.

#### **1-5 over view of the study**

This study is concerned with characterization of benign and malignant liver lesions using ultrasound and texture analysis. It falls five chapters. Chapter one is an introduction which includes introductory notes on the focal liver lesions and study objectives as well as statement of the problem , while chapter tow will include anatomy, physiology ,pathology of the liver , literature reviews concerning the previous study , ultrasound technique of the liver and son graphic appearance of focal liver lesions . Then chapter three deal with methodology, where it provides an outline of material and methods used to acquire the data in the study as well as the method of analysis approach. While the results were presented in chapter four. And finally chapter five include discussion of the results, conclusions and recommendation, followed by reference and appendices.

## Chapter two

### Background and literature review

#### 2-1 Anatomy:

The liver is the largest of the abdominal viscera, occupying a substantial portion of the upper abdominal cavity. It occupies most of the right hypo chondrium and epigastrium, and frequently extends into the left hypochondrium as far as the left lateral line (**Fig. 2.1**). As the body grows from infancy to adulthood the liver rapidly increases in size. This period of growth reaches a plateau around 18 years and is followed by a gradual decrease in the liver weight from middle age. The liver weighs approximately 5% of the body weight in infancy and it decreases to approximately 2% in adulthood. The size of the liver also varies according to sex, age and body size. It has an overall wedge shape. The narrow end of the wedge lies towards the left hypochondrium and the anterior edge points interiorly and inferiorly. The superior and right lateral aspects are shaped by the anterolateral abdominal and chest wall as well as the diaphragm. The inferior aspect is shaped by the adjacent viscera. (**Suzan 2008**)

Throughout life the liver is reddish brown in color, although this can vary depending upon the fat content. Obesity is the most common cause of excess fat in the liver (also known as steatosis): the liver assumes a more yellowish tinge as its fat content increases. The texture's usually soft to firm, although it depends partly on the volume of blood the liver contains and the fat content. . (**Suzan 2008**)

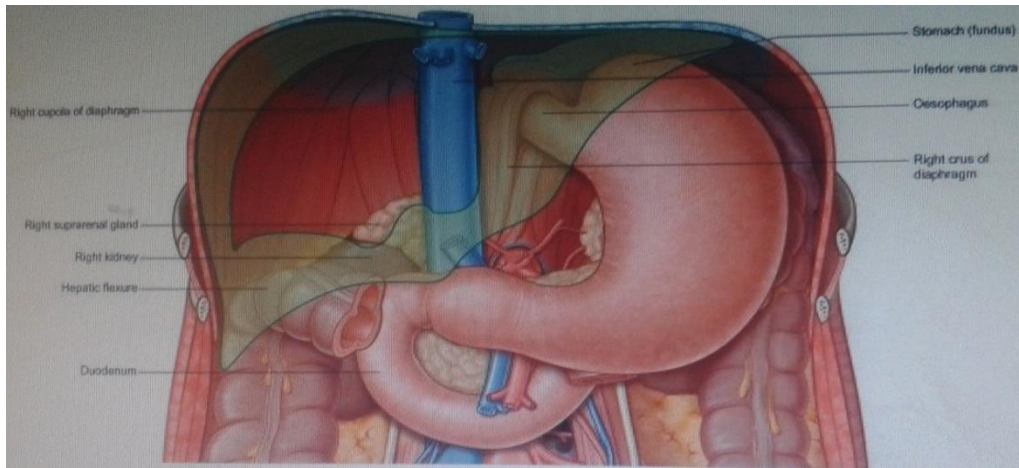


**Figure. (2-1)The bed of the liver, the outline of the liver is shaded green. The central pair area is unshaded ( Gray's anatomy)**

### **2-1-1 Surfaces of the liver**

The liver is usually described as having superior, anterior, right, posterior and inferior surfaces, and has a distinct inferior border. **(Fig, 2.2)**

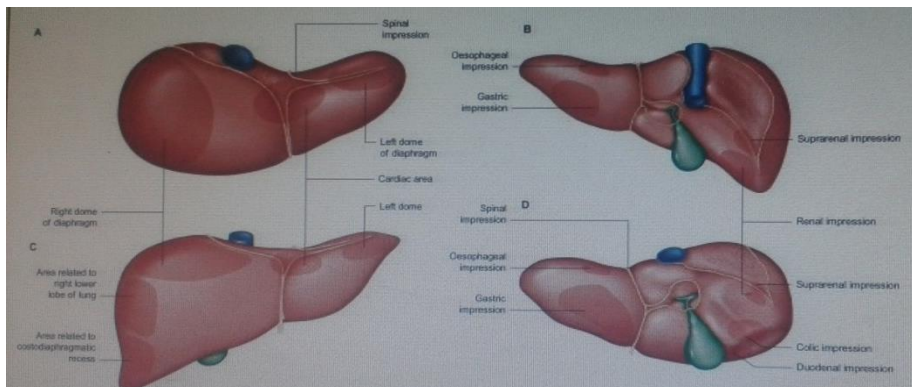


**Figure.(2-2)Relations of the liver, A, superior view, B, posterior view, C, anterior view, D, inferior view. (Gray's anatomy)**

#### **2-1-1-1 Superior surface**

The superior surface is the largest surface and lies immediately below the diaphragm, separated from it by peritoneum except for a small triangular area where the two layers of the falciform ligament diverge. The majority of the superior surface lies beneath the right dome, but there is a shallow cardiac

impression centrally that corresponds to the position of the heart above the central tendon of the diaphragm. (Suzan 2008)

#### **2-1-1-2 Anterior surface**

The anterior surface is approximately triangular and convex and is covered by peritoneum except at the attachment of the falciform ligament. Much of it is in contact with the anterior attachment of the diaphragm. (Suzan 2008)

#### **2-1-1-3 Right surface**

The right surface is covered by peritoneum and lies adjacent to the right dome of the diaphragm which separates it from the right lung and pleura and the seventh to 11th ribs. (Suzan 2008)

#### **2-1-1-4 Posterior surface**

The posterior surface is convex, wide on the right, but narrow on the left . Much of the posterior surface is attached to the diaphragm by loose connective tissue, forming the triangular 'bare area'. The inferior vena cava lies in a groove or tunnel in the medial end of the 'bare area'. To the left of the caval groove the posterior surface of the liver is formed by the caudate lobe, and covered by a layer of peritoneum continuous with that of the inferior layer of the coronary ligament and the layers of the lesser omentum. (Suzan 2008)

#### **2-1-1-5 Inferior surface**

The inferior surface is bounded by the inferior edge of the liver. It blends with the posterior surface in the region of the origin of the lesser omentum, the porta hepatis and the lower layer of the coronary ligament, and is marked near the midline by a sharp fissure which contains the ligamentum teres (the obliterated fetal left umbilical vein). The quadrate lobe lies between the fissure for the ligamentum teres and the gallbladder.

The inferior surface of the left lobe is related inferiorly to the fundus of the stomach and the upper lesser omentum. The quadrate lobe lies adjacent to the

pylorus, first part of the duodenum and the lower part of the lesser omentum. **(Suzan 2008).**

### **2-1-2 Gross anatomical lobe**

Historically, the liver has been considered to be divided into right, left, caudate and quadrate lobes by the surface peritoneal and ligamentous attachments. **(Suzan standring 2008).**

#### **2-1-2-1 Right lobe**

The right lobe is the largest in volume and contributes to all surfaces of the liver. It is divided from the left lobe by the falciform ligament superiorly and the ligamentum venosum inferiorly. The caudate lobe lies posterior, and the quadrate lobe anterior, to the porta hepatis. The gallbladder lies in a shallow fossa to the right of the quadrate lobe. **(Suzan 2008)**

#### **2-1-2-2 Left lobe**

The left lobe is the smaller of the two main lobes, although it is nearly as large as the right lobe in young children.

It lies to the left of the falciform ligament with no subdivisions, and is substantially thinner than the right lobe, having a thin apex that points into the left upper quadrant. **(Suzan 2008)**

#### **2-1-2-3 Quadrate lobe**

The quadrate lobe is visible as a prominence on the inferior surface of the liver, to the right of the groove formed by the ligamentum venosum (and thus is incorrectly said to arise from the right lobe although it is functionally related to the left lobe). It lies anterior to the porta hepatis and is bounded by the gallbladder fossa to the right, a short portion of the inferior border anteriorly, the fissure for the ligamentum teres to the left, and the porta hepatis posteriorly. **(Suzan 2008)**



#### **2-1-2-4 caudate lobe**

The caudate lobe is visible as a prominence on the inferior and posterior surfaces to the right of the groove formed by the ligamentum venosum: it lies posterior to the porta hepatis. To its right is the groove for the inferior vena cava. Above it continues into the superior surface on the right of the upper end of the fissure for the ligamentum venosum. in gross anatomical description this lobe said to arise from right lobe , but functionally separate . **(Suzan 2008)**

#### **2-1-3 Functional anatomy**

Current understanding of the functional anatomy of the liver is based on Cournand's division of the liver into eight (subsequently nine) functional segments, based upon the distribution of portal venous branches and the location of the hepatic veins in the parenchyma (Cournand 1957). Further understanding of the intrahepatic biliary anatomy, especially of the right ductal system, was enhanced by contributions from Hjortsjo (1948) and Healey & Schroy (1953) using the biliary system as the main guide for division of the liver **(Fig. 2.3)**. **(Suzan standring 2008)**

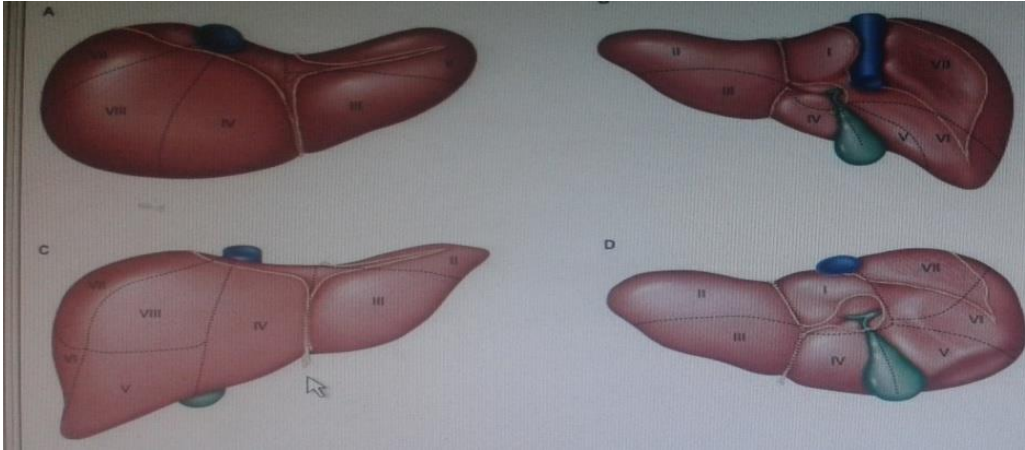


**Figure. (2-3) Segments of the liver (after Couinaud) A, superior view, B, posterior view, C, interior view, D, inferior view. The segments are sometimes referred to by number (name) – 1 (caudate) (sometimes subdivided into left and right parts called segment IX); II (left lateral superior), III (left medial inferior), IV (left medial superior) (sometimes subdivided into superior and inferior parts), V (right medial inferior), VI (right lateral inferior), VII (right lateral superior), VIII (right medial superior). . (Gray's anatomy)**

#### **2-1-4 Sectors and segments of the liver**

The sectors of the liver are made up of between one and three segments: right lateral sector = segments VI and VII; right medial sector = segments V and VIII; left medial sector = segments III and IV (and part of I); left lateral sector = segment II (**Fig. 2.3**).

Segments are numbered in an anti-clockwise spiral centered on the portal vein with the liver viewed from beneath, starting with segment I up to segment VI, and then back clockwise for the most cranial two segments VII and VIII (**Suzan 2008**)

#### **2.1.4.1 Segment I**

Segment I corresponds to the anatomical caudate lobe and lies posterior (dorsal) to segment IV with its left half directly posterior to segments II and II and its medial half surrounded by major vascular branches. the segment therefore receives vessels independently from the left and right portal veins and hepatic arteries, and it drains independently into the inferior vena cava by multiple small branches (referred to as the lower group). **(Suzan standring 2008)**

#### **2.1.4.2 Segment II**

Segment II is the only segment in the left lateral sector of the liver and lies postero-lateral to the left fissure. It often has only one Glissonian sheath and drains into the left hepatic vein. Rarely, a separate vein drains directly into the inferior vena cava. **(Suzan standring 2008)**

#### **2.1.4.3 Segment III**

Segment III lies between the umbilical fissure and the left fissure and is often supplied by one to three Glissonian sheaths: it drains into the left hepatic vein. The vein of the falciform ligament can provide an alternative drainage route for segment III. **(Suzan standring 2008)**

#### **2.1.4.4 Segment IV**

Segment IV lies between the umbilical fissure and the main fissure, anterior to the dorsal fissure and segment I. Segment IV is supplied by three to five Glissonian sheaths, of which the majority arises in the umbilical fissure; their origins are often close to those that supply to segments II and III. Occasionally segment IV is supplied by branches from the main left pedicle. The main venous drainage segment is into the middle hepatic vein; the segment can also drain into the left hepatic vein through the vein of the falciform ligament. **(Suzan standring 2008)**

#### **2.1.4.5 Segment V**

Segment V is the inferior segment of the right medial sector and lies between the middle and the right hepatic veins. Its size is variable, as are the number of Glissonian sheaths that supply it. Venous drainage is into the right and middle hepatic veins. **(Suzan standring 2008)**

#### **2.1.4.6 Segment VI**

Segment VI forms the inferior part of the right lateral sector posterior to the right portal fissure. It is often supplied by two to three branches from the right posterior Glisson's sheath, but occasionally the Glisson's sheath to segment VI can arise directly from the right pedicle. Venous drainage is normally into the right hepatic vein, but may be via the right inferior hepatic vein directly into the inferior vena cava. **(Suzan standring 2008)**

#### **2.1.4.7 Segment VII**

Segment VII forms the superior part of the posterior sector and lies behind the right hepatic vein. The sheaths to segment VII are often single. The venous drainage is into the right hepatic vein; occasionally the segment can drain through the right middle hepatic vein directly into the inferior vena cava. **(Suzan standring 2008)**

#### **2.1.4.8 Segment VIII**

Segment VIII is the superior part of the right anterior sector. The right anterior sectoral sheaths end in segment VIII and supply it after giving off branches to segment V. The venous drainage is to the right and middle hepatic veins. **(Suzan standring 2008)**

#### **2.1.4.9 Segment IX**

Segment IX is a recent subdivision of segment I, and describes that part of the segment that lies posterior to segment VIII. **(Suzan standring 2008)**

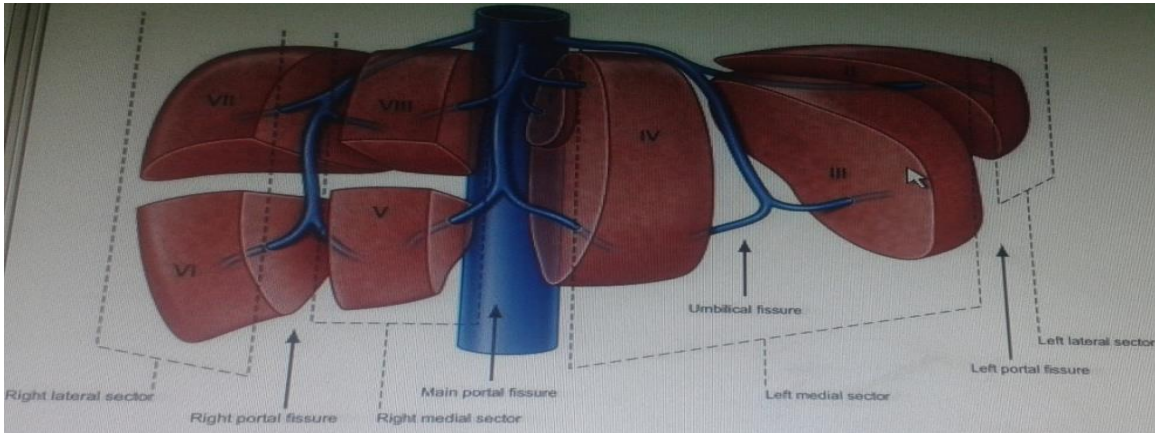


**Figure. (2-3) The fissures and sectors of the liver. (Right lateral = right posterior; right medial = right anterior.) . (Gray’s anatomy)**

### **2-1-5 Fissures of the liver**

Knowledge of the fissures of the liver is essential for understanding liver surgery. Three major fissures, not visible on the surface, run through the liver parenchyma and harbor the three main hepatic veins (main, left and right portal fissures). Three minor fissures are visible as physical clefts of the liver surface (umbilical, venous and fissure of Gans). (fig 2-3)(Suzan 2008)

#### **2-1-5-1 Main portal fissure**

The main fissure extends from the tip of the gallbladder back to the midpoint of the inferior vena cava and contains the middle (main) hepatic vein. It separates the liver into right and left hemi-livers. Segments V and VIII lie to the right and segment IV to the left of the fissure. (Suzan 2008)

#### **2-1-5-2 Left portal fissure**

The left fissure divides the left hemi-liver into medial (anterior) and lateral (posterior) sectors. It extends from the midpoint of the anterior edge of the liver between the falciform ligament and the left triangular ligament to the point which

marks the confluence of the left and middle hepatic veins. It contains the left hepatic vein and separates the left anterior and left posterior sectors: segment III lies anteriorly and segment II posteriorly. (**Suzan 2008**)

### **2-1-5-3 Right portal fissure**

The right portal fissure divides the right hemi-liver into lateral (posterior) and medial (anterior) sectors. The fissure divides the right anterior sector to its left (segments V and VIII) from the right posterior sector to its right (segments VI and VII), and contains the right hepatic vein. The right fissure marks the thickest point of liver parenchyma which is commonly transected during liver resection. (Suzan standing 2008)

### **2-1-5-4 Umbilical fissure**

The umbilical fissure separates segment III from segment VI within the left anterior sector and contains a main branch of the left hepatic vein (the umbilical fissure vein). It is marked by the attachment of the falciform ligament and sometimes covered by a ridge of liver tissue extending between the segments. (**Suzan 2008**)

### **2-1-4-5 Venous fissure**

The venous fissure is a continuation of the umbilical fissure on the under surface of the liver and contains the ligamentum venosum. It lies between the caudate lobe and segment IV. (**Suzan 2008**)

### **2-1-5-6 Fissure of Gans**

The fissure of Gans lies on the undersurface of the right lobe of the liver behind the gallbladder fossa. It often contains the portal pedicle to the right posterior sector and is thought to correspond to the right fissure as it relates to the separation of the sectors of the liver. (**Suzan 2008**)

## **2-1-6 vascular supply and lymphatic drainage**

The vessels connected with the liver are the portal vein, hepatic artery and hepatic veins. The portal vein and hepatic artery ascend in the lesser omentum to the porta hepatis, where each bifurcates. The hepatic bile duct and lymphatic vessels descend from the porta hepatis in the same omentum . The hepatic veins leave the liver via its posterior surface and run directly into the inferior vena cava. **(fig 2-6)**  
**(Suzan 2008)**

### **2-1-6-1 Hepatic artery**

In adults the hepatic artery is intermediate in size between the left gastric and splenic arteries. In fetal and early postnatal life it is the largest branch of the celiac axis. The hepatic artery gives off right gastric, gastro duodenal and cystic branches as well as direct branches to the bile duct from the right hepatic and sometimes the supra duodenal artery . After its origin from the celiac axis, the hepatic artery passes inferiorly and laterally below the epiploic foramen to the upper aspect of the first part of the duodenum. It may be subdivided into the common hepatic artery, from the celiac trunk to the origin of the gastro duodenal artery, and the hepatic artery 'proper', from that point to its bifurcation. It passes anterior to the portal vein and ascends anterior to the epiploic foramen between the layers of the lesser omentum. **(Suzan 2008)**

### **2-1-6-2 Veins**

The liver has two venous systems. The portal system conveys venous blood from the majority of the gastrointestinal tract and its associated organs to the liver . The hepatic venous system drains blood from the liver parenchyma into the inferior vena cava. **(Suzan 2008)**

#### **2-1-6-2-1 Portal vein**

The portal vein begins at the level of the second lumbar vertebra and is formed from the convergence of the superior mesenteric and splenic veins. It is

approximately 8 cm long and lies anterior to the inferior vena cava and posterior to the neck of the pancreas.

It enters the right border of the lesser omentum, ascends anterior to the epiploic foramen to reach the right end of the porta hepatis and then divides into right and left main branches which accompany the corresponding branches of the hepatic artery into the liver. In the lesser omentum the portal vein lies posterior to both the common bile duct and hepatic artery. It is surrounded by the hepatic nerve plexus and accompanied by many lymph vessels and some lymph nodes.

#### **2-1-6-2-2 Hepatic veins:**

The liver is drained by three major hepatic veins into the supra hepatic part of the inferior vena cava and a multitude of minor hepatic veins that drain into the intra hepatic inferior vena cava. The three major veins are located between the four major sectors of the liver .which are Right hepatic vein, Middle hepatic vein, Left hepatic vein and Minor veins **Fig (2.5). (Suzan 2008)**



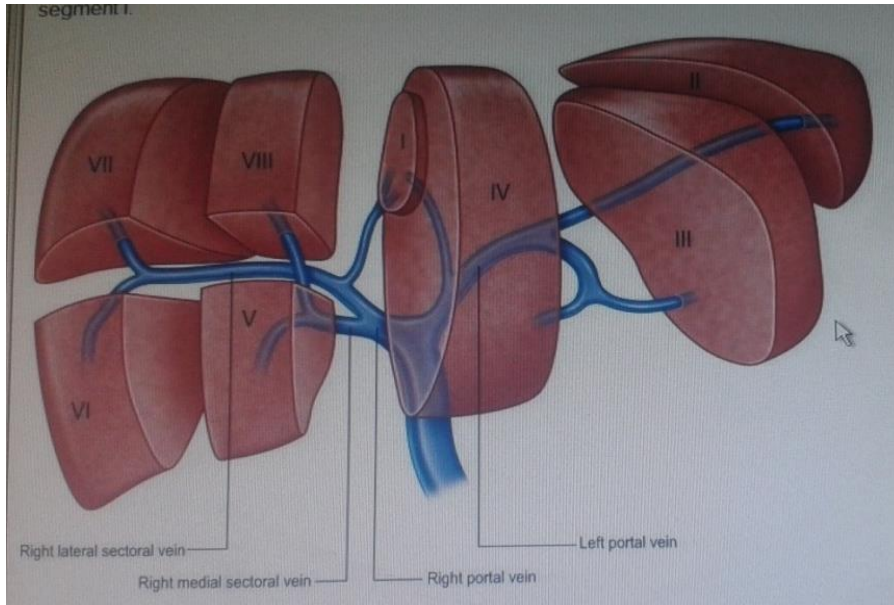


**Figure. (2-5)** The main portal vein and its intra hepatic branches. (Right lateral = right posterior; right medial = right anterior. **(Gray's anatomy)**)

### **2-1-6-3 Lymphatic's**

Lymph from the liver has abundant protein content. Lymphatic drainage from the liver is wide and may pass to nodes above and below the diaphragm. Obstruction of the hepatic venous drainage increases the flow of lymph in the thoracic duct. Hepatic collecting vessels are divided into superficial and deep systems. **(Suzan 2008)**

### **2-2 Physiology**

The structural unit of the liver is the liver lobule, roughly hexagocolumn of liver cells (hepatocytes). Between adjacent lobules are branches of the hepatic artery and portal vein. The capillaries of a lobule are sinusoids, large and very permeable vessels between the rows of liver cells. The sinusoids receive blood from both the hepatic artery and portal vein, and it is with this mixture of blood that the liver cells carry out their functions. The hepatic artery brings oxygenated blood, and the

portal vein brings blood from the digestive organs and spleen. Each lobule has a central vein. The central veins of all the

lobules unite to form the hepatic veins, which take blood out of the liver to the inferior vena cava. The cells of the liver have many functions but their only digestive function is the production of bile. The Bile enters the small bile ducts, called bile canaliculated, on the liver cells, which unite to form larger ducts and finally merge to form the hepatic duct, which takes bile out of the liver. The hepatic duct unites with the cystic duct of the gallbladder to form the common bile duct, which takes bile to the duodenum. Bile is mostly water and has an excretory function in that it carries bilirubin and excess cholesterol to the intestines for elimination in feces. The digestive function of bile is accomplished by bile salts, which emulsify fats in the small intestine. Emulsification means that large fat globules are broken into smaller globules. This is mechanical, not chemical, digestion; the fat is still fat but now has more surface area to facilitate chemical digestion. Production of bile is stimulated by the hormone secretin, which is produced by the duodenum when food enters the small intestine. **(Scanlon 2008)**

The liver is a remarkable organ, and only the brain is capable of a greater variety of functions. The liver cells (hepatocytes) produce many enzymes that catalyze many different chemical reactions. These reactions are the functions of the liver. As blood flows through the sinusoids (capillaries) of the liver, materials are removed by the liver cells, and the products of the liver cells are secreted into the blood. Because the liver has such varied effects on so many body systems.

### **2-2-1 Carbohydrate metabolism**

The liver regulates the blood glucose level by convert the excess glucose to glycogen (glycogen sis) when the blood glucose is high; the hormones insulin and cortisol facilitate this process. During hypoglycemia or stress situations, glycogen is converted back to glucose (glycogenolysis) to raise the blood glucose level. Epinephrine and glucagon are the hormones that facilitate this process. The liver also changes other monosaccharide to glucose. Fructose and galactose, for example, are end products of the digestion of sucrose and lactose.

Because most cells, however, cannot readily use fructose and galactose as energy sources, they are converted by the liver to glucose, which is easily used by cells.

**(Scanlon 2008)**

### **2-2-2 Amino acid metabolism**

The liver regulates blood levels of amino acids based on tissue needs for protein synthesis. Of the 20 different amino acids needed for the production of human proteins, the liver is able to synthesize 12, called the nonessential amino acids. The chemical process by which this is done is called transamination, The transfer of amino group (NH<sub>2</sub>) from an amino acid present in excess to a free carbon chain that forms a complete, new amino acid molecule. The other eight amino acids, which the liver cannot synthesize, are called the essential amino acids. In this case, “essential” means that the amino acids must be supplied by our food, because the liver cannot manufacture them. Similarly, “non-essential” means that the amino acids do not have to be supplied in our food because the liver can make them. All 20 amino acids are required in order to make our body proteins. Excess amino acids, those not needed right away for protein synthesis, cannot be stored. However, process of domination, which also occurs in the liver, the NH<sub>2</sub> group is removed from an amino acid, and the remaining carbon chain may be converted to a simple carbohydrate molecule or to fat. Thus, excess amino acids are utilized for

energy production: either for immediate energy or for the potential energy stored as fat in adipose tissue. The NH<sub>2</sub> groups that were detached from the original amino acids are combined to form urea, a waste product that will be removed from the blood by the kidneys and excreted in urine. (Scanlon 2008)

### **2-2-3 Lipid metabolism**

The liver forms lipoproteins, which as their name tell us, are molecules of lipids and proteins, for the transport of fats in the blood to other tissues. The liver also synthesizes cholesterol and excretes excess cholesterol into bile to be eliminated in feces. Fatty acids are a potential source of energy, but in order to be used in cell respiration they must be broken down to smaller molecules. (Scanlon 2008)

### **2-2-4 Synthesis of plasma proteins**

The liver synthesizes many of the proteins that circulate in the blood. Albumin, the most abundant plasma protein, helps maintain blood volume by pulling tissue fluid into capillaries. The clotting factors are also produced by the liver. These, as you recall, include prothrombin, fibrinogen, and Factor 8, which circulate in the blood until needed in the chemical clotting mechanism. The liver also synthesizes alpha and beta globulins, which are proteins that serve as carriers for other molecules, such as fats, in the blood. (Scanlon 2008)

### **2-2-5 Formation of bilirubin**

The liver contains fixed macrophages that phagocytize old red blood cells (RBCs). Bilirubin is then formed from the heme portion of the hemoglobin. The liver also removes from the blood the bilirubin formed in the spleen and red bone marrow and excretes it into bile to be eliminated in feces. (Scanlon 2008)

### **2-2-6 Phagocytosis by Kupffer cells**

The fixed macrophages of the liver are called (Kupffer cells). Besides destroying old RBCs, Kupffer cells phagocytise pathogens or other foreign material that circulate through the liver. Many of the bacteria that get to the liver come from the

colon. These bacteria are part of the normal flora of the colon but would be very harmful elsewhere in the body. The bacteria that enter the blood with the water absorbed by the colon are carried to the liver by way of portal circulation. The Kupffer cells in the liver phagocytize and destroy these bacteria, removing them from the blood before the blood returns to the heart. **(Scanlon 2008)**

### **2-2-7 Storage**

The liver stores the fat-soluble vitamins A, D, E, and K, and the water-soluble vitamin B12. Also stored by the liver are the minerals iron and copper. You already know that iron is needed for hemoglobin and myoglobin and enables these proteins to bond to oxygen. Copper (as well as iron) is part of some of the proteins needed for cell respiration, and is part of some of the enzymes necessary for hemoglobin synthesis. **(Scanlon 2008)**

### **2-2-8 Detoxification**

The liver is capable of synthesizing enzymes that will detoxify harmful substances, That is, change them to less harmful ones. Alcohol, for example, is changed to acetate, which is a two carbon molecule (an acetyl group) that can be used in cell respiration. Medications are all potentially toxic, but the liver produces enzymes that break them down or change them. When given in a proper dosage, a medication exerts its therapeutic effect but is then changed to less active substances that are usually excreted by the kidneys. An overdose of a drug means that there is too much of it for the liver to detoxify in a given time, and the drug will remain in the body with possibly harmful effects. This is why alcohol should never be consumed when taking medication. **(Scanlon 2008)**

### **2-3 Over view of texture analysis methods**

Texture analysis provides many important discriminating characteristics, not normally perceptible with visual inspection .with probably chosen with (TA) methods ,an-image –based diagnosis could be considerably improved.

Different medical imaging modalities are presently available to assist clinicians in detection and diagnosis of human pathologies. Among these are computed tomography, proton emission tomography, magnetic resonance imaging and ultrasonography. With a contrast improvement of image acquisition devices the amount of diagnostic information obtained in a single study has considerably increased. In such a situation, interpretation of image content based on its visual inspection goes far beyond the human abilities. The human eye can distinguish barely 100 gray levels, where the gray-scale images obtained nowadays (still commonly used) can encode many thousands of gray levels. **(Dorota 2014)**

Since an experienced physician is not able to read all the useful imaging data without any additional equipment, a great deal of work has been devoted to develop different methods for (semi-) automatic medical image analysis, interpretation, and recognition. As a result, many computer-aided diagnosis (CAD) systems have been proposed over the past two decades. These systems combine a broad range of image analysis methods (including image segmentation and tissue characterization techniques), feature selection and classification algorithms.

The advantage of (CAD) systems improved considerably the image-based diagnoses which reduces the necessity of using other methods, such as a fine-needle aspiration biopsy. Moreover, medical imaging is becoming continuously cheaper, faster and less wasteful. Finally it is certainly much less invasive. In comparison with many gold standard procedures.

In 1979, Haralik stated that one of the most important sources of analyzed image region could be its texture. **(Harilik 1979)**

It characterizes the spatial relationships between gray levels describing pixels within a considered image region (so called Region of interest, commonly abbreviated as ROI) since then numerous review studies have

Shown that texture analysis could be highly useful in various problems related to the recognition of medical images. (**Cendes et al 2010** ) and (**Kssner & Thornhill 2010**)

As it provides a crucial information in terms of tissue discrimination. Moreover, many work have revealed that digital image analysis enables to detect the high order texture properties not accessible to visual inspection,

Three main textural analysis approaches are considered: statistical, model-based, and filterer-based. (**Dorota Duda 2014**)

The different texture analysis methods described as follows:

### **2-3-1 Gray level histogram**

Features derives from a gray level histogram (GLH) are based on the distribution of pixel gray levels and do not consider the relationship between neighboring pixels. They provide knowledge on the most and the less often occurring gray levels, on the concentration of the gray levels around their average, or on the degree of asymmetry in their distributions. on contrary, they do not contain any information neither about the possible direction of the texture , nor about its structure .nevertheless they are often used because of their invariability to translation or rotation, simplicity, and low memory and time requirements of their calculation. the most popular first-order features are:

Range of gray levels, Mean of gray levels (measure of image brightness), Median gray level (the second quartile), Gray level energy (indicates how the gray levels are distributed), Variance of gray levels (characterizes the distribution of gray level around

the mean), Gray level skewness (measures the asymmetry of the gray level histogram), Gray level kurtosis (indicate the relative flattening of the gray level histogram), Co-officience of variation (the ratio of the standard deviation to the mean). (**Dorota 2014**)

### **2-3-2 Co – Occurrence Matrices**

Co-Occurrence Matrices (COM) were introduced by Haralick et al. This method consists in analyzing all possible pairs of pixels, space apart by a fixed distance. Several texture characteristics can be obtained on the basis of a co-occurrence matrix: **(Dorota) 2014**

Energy or angular second moment (measure of homogeneity of gray levels characterizing the pixels within an analyzed region of interest), Contrast or inertia (measure of contrast or local variations in pixel gray level), Inverse difference moment (measure of local homogeneity), Entropy (quantifies a degree of randomness of the pixel gray level), Correlation (measures linear dependency of gray level on neighboring pixel).

Other features can be calculated from sum of probabilities that relate to specified intensity sum or differences **(Bankman2008)**

this requires the construction of vectors whose components are the co-occurrence probabilities of pairs of pixels with a determined sum or difference of gray levels.

Some features derived from such vectors are :

Sum average, sum variance, sum entropy. Difference average, difference variance, and difference entropy. **(Dorota) 2014**

### **2-3-3 Run Length Matrix**

Run length matrix (RLM) features are based on probabilities of pixel runs of each possible length arranged in a certain direction **(GALLOWAY 1975)**

Galloway initially proposed the following features, derived from a run length matrix:

Short run emphasis, long run emphasis, gray level non-uniformity. (Distribution), run length non-uniformity (distribution), and fraction of image in runs.

The possibilities of two additional features are:



low gray level runs emphasis, high gray level runs emphasis, and run length entropy. (Dorota 2014)

### 2-3-4 Gray Level Difference Matrix

Gray level Difference Matrices (GLDM) are constructed with consideration of only the absolute values of differences between the gray levels of pixels, still considered in pairs (Rosenfeld, A et al 1976)

all possible absolute differences in gray levels that can be encoded in the image are taken into account. For each absolute difference, the probability of finding a pair of pixels with just such a difference in the gray levels is calculated. The probabilities are sorted in increasing order of corresponding absolute gray differences from a vector  $I(d,0) = (I_0, I_1, \dots, I_{G-1})^T$ , where  $G$  is the number of gray levels possible to be encoded in an image.

five texture features can be derived from the  $I(d, \Theta)$  vector:

Mean (measures a level of texture diversity), Energy or angular second moment (measure of homogeneity of gray levels), Contrast or inertia (measure of intensity contrast between a pixel and its neighbors), Inverse difference moment (measure of local homogeneity), Entropy (quantifies a degree of randomness of the pixel gray levels). (Dorota 2014)

### 2-3-5 Gradient Matrices

Gradient-based features were introduced by Lerski et al. A gray-level gradient at a particular image point is a function of the difference between the gray levels of its neighboring pixels, aligned in a vertical and horizontal line passing through the point. The gradient matrix (GM) contains the values of the absolute gradients at each point of an analyzed image region, excluding its boundaries.

Features derived from a gradient matrix are the following:

mean, variance, skewness, kurtosis, and percentage of pixels with non zero gradient.

They can provide the information on the uniformity, homogeneity, or the roughness of the texture. They may also indicate the presence or absence of edges.

**.(Dorota ) 2014**

### **2-3-6 Texture Feature Coding Method**

Texture Feature Coding Method (TFCM) was proposed by Horng et al.

The method consists of three steps:

**First**, an image is transformed.

The transformation consists of assigning to each pixel (except for the pixels located at the edges of a considered ROI) a value that measures a degree of heterogeneity (of variation, of diversity) of the local gray levels of its neighbors. this measure called a "Texture Feature Number" (TFN). Only a neighborhood of 3\_3 pixels is considered.

**Afterwards**, a histogram of Texture Feature Numbers and co-occurrence matrices are constructed, based on a transformed,

**finally** several texture descriptors are obtained, either from a TFN histogram:

– coarseness, homogeneity, mean convergence (indicates how close the texture approximates the mean), variance (measures deviation of TFNs from the mean), either from a TFN-based co-occurrence matrix:entropy,code similarity (assesses the density of the same TFNs in a 3x3 neighborhood), resolution similarity (measures the local homogeneity of TFNs). ( **Horng et al.2002**)

### **2-3-7 Autocorrelation Coefficients**

Autocorrelation Coefficients (AC) expresses the correlation of the gray levels describing pixels within a defined neighborhood. It is the function of the vertical (Dx) and the horizontal (Dy) distance between the considered pixels in pairs. Usually such distances are relatively small. In order to normalize the autocorrelation co-efficient a gray level of each pixel is decreased by the mean

gray level. Normalized auto correlation coefficients are independent of the image brightness, and can be regarded as textural features. They can provide knowledge on the spatial relationship between the texture patterns, and the average size of texture patterns. (**Gonzalez, R.C.&Woods, R.E 2002**)

### **2-3-8 Fractal Model (FM)**

Fractal Model (FM) was described in several works . Mandelbrot characterized fractals as self-similar objects, whose parts are similar to the whole, and whose topological dimension is not an integer (**Mandelbrot1982**) . The fractal dimension of an object reflects the extent to which this object fills the space or the rate of its diversity, the degree of irregularity of the object .A gray-level image can be considered as a topographic surface in three dimensional space, where two dimensions are those of the image plane and the third one (height) is the gray level of image pixels. The fractal dimension of such a surface can be used as a texture descriptor. It can measure the irregularity and the roughness of the texture. Irregular surfaces (corresponding to diversified textures) have relatively high fractal dimension, while the smooth ones are characterized by the low fractal dimension. (**Dorota 2014**)

### **2-3-9 Discrete Wavelet Transform**

Discrete Wavelet Transform (DWT) of an image consists in its convolution with two filters, the low-pass and the high-pass one, separately throughout the image rows and separately throughout the image columns.(**Dorota 2014**). The Mallat algorithm for DWTdivides the image into the four sub-images, each of which is linearly two times smaller than the decomposed image. Each sub-image can then be divided in the same manner .Thus multiple resolution levels are obtained. Four sub-band images created at each decomposition step are denoted:  $d_{LL}$  ,  $d_{LH}$  ,  $d_{HL}$  , and  $d_{HH}$ . They are created by applying, respectively: the low-pass filter for

rows and columns (LL), the low-pass filter for rows and the high-pass filter for columns (LH), the high-pass filter for rows and the low-pass filter for columns (HL), the low-pass filter for rows and columns (LL). The component dLL is created by calculating the average of disjoint groups of 2\_2 pixels, using Haar transform. It is therefore an approximation (simplified representation) of the transformed image. Further sub-bands represent the vertical (LH), the horizontal (HL) and the diagonal (HH) image information. On the basis of the mean edge energy at three directions can be calculated. It is also possible to analyze the energy distribution in each sub-band image. The image dLL is used only for DWT calculation at the next scale. (Mallat, S.G 1989)

### **2-3-10 Laws' Texture Energy measures**

Laws' Texture Energy (LTE) measures [65] are useful for estimating the frequency of the image elements, such as ripples, edges, or spots. Laws proposed to transform the images using linear filters. During the transformation, each image pixel is assigned a value that is a combination of initial gray levels of pixels belonging to a neighborhood of a transformed pixel. Usually two types of neighborhood are considered: 3\_3 pixels and 5\_5 pixels. The weights of the neighboring pixels are defined by a zero sum

Convolution matrix (so-called Laws' mask). For each pair of asymmetric masks, the resulting images could be added. In this case, images obtained with an application of symmetric masks are multiplied by two. On the basis of a transformed image, the entropy can be calculated. Also, the filtered images can be once again subjected to further transformation, that results in creation of texture energy images. Finally, the features such as: mean, variance, skewness, and kurtosis can be calculated from the resulting images. (Laws, K.I 1980)

## **2-4 Liver lesions:**

Liver lesions represent a heterogeneous group of pathology ranging from solitary benign lesions to multiple metastases from a variety of malignant tumors.

Liver lesions maybe infiltrative or has mass effect. Be solitary or multiple, benign or malignant.

Assessment of liver lesions takes into considerate their appearance on a variety of imaging modalities and their vascularity: Cystic liver lesions. Hyper vascular liver lesions and Liver tumors. (Dr Jeremy etal.2014)

### **2-4-1 Cystic liver lesions:**

Cystic liver lesions carry a broad differential diagnosis, these include:-

**Simple cysts:** includes:

Simple hepatic cyst, biliary hamartoma, carols disease, and adult polycystic liver disease.

### **Infectious inflammatory conditions**

**Hepatic abscesses** include:

Pyogenic hepatic abscess, amoebic hepatic abscess, and fungal abscess.

Hepatic hydated cyst.

Neoplastic tumors includes

Biliary cyst adenoma. Biliary cyst adenocarcinomas and cystic hepatic metastases.

( Dr Yuranga et al 2106)

#### **2-4-1-1 Simple cysts**

##### **2-4-1-1-1 Simple hepatic cyst**

Simple hepatic cysts are commonest benign liver lesions and have no malignant potential they can be diagnosed by Ultrasound, CT or MRI.

There may be a slight female predilection. It may be isolated or multiple and may vary from a few millimeters to several centimeters in diameter simple hepatic cysts are benign developmental lesions that do not communicate with the biliary

tree., they originate from hamartomatous tissue .on histopathological analysis true hepatic cysts contain serous fluid and are lined by an early imperceptible wall consisting of cuboidal epithelium, identical it that of the bile ducts and a thin underlying rim of fibrous seroma. While they can occur anywhere in the liver they maybe a greater predilection towards the right lobe the liver. **.(Dr Yuranga et al 2106)**

On ultrasound they appear as :

Round or ovoid anechoic lesion (maybe lobulated) , well-marginated with a thin or imperceptible wall and clearly defined back wall , it may show posterior a caustic enhancement if large enough .a few septa maybe possible but no wall thickening, a small amount of layering debris is possible. No internal vascularity on color Doppler .( **DrYuranga et al 2016**)

#### **2-4-1-1-2 Multiple Biliary hamartomas:**

Multiple biliary hamartoma (MBH) are a rare cause of multiple benign hepatic lesions. It also known as Von Meyenburg Complexes.

Biliary hamartoma are composed of small disorganized clusters of dilated cystic bile ducts lined by a single layer of cuboidal cellsand surrounded by an abundant fibro collage nous stroma. They are thought to arise from embryonic bile duct remnants that have failed to involutes. On ultrasound they appear as small round or irregular lesions and are usually echogenic if discreetly seen, often tiny individual hamartoma cannot be resolved and are instead interpreted as diffuse heterogeneous liver echo texture , larger hamartoma less than 10mm may appear hypo echoic or anechoic and commit tail artifact maybe seen . **(Dr Andrew et al 2016)**

#### **2-4-1-1-3 Caroli disease:**

Caroli disease is a congenital disorder comprising of multifocal cystic dilatation of segmental intrahepatic bile ducts .

Caroli disease is a rare autosomal recessive disorder which has no recognized gender predilection. It belongs to the spectrum of fibro polycystic liver disease which results from utero malformation of the ductal plate.

The ductal plate is a layer of hepatic precursor cells that surround the portal venous branches. And is the angle of the intrahepatic ducts thus the simple type of Caroli disease results from the abnormal development of the large bile ducts. **.(Dr Henry ,and Dr Alexandra et al)**

On ultrasound may show dilated intrahepatic bile duct(IHBD) , intra ductal bridging : echogenic septa traversing the dilated bile duct lumen .small portal venous branches partially or completely surrounded by dilated bile ducts, and intraductal calculi.**( Dr Alexandra et al 2016)**

#### **2-4-1-1-4 Adult polycystic liver disease (PCLD):**

Is a heredity condition that arise either in patient with autosomal dominant polycystic kidney disease (ADPCKD),or in a patient with a different genetic mutation that results solely in autosomal polycystic liver disease. It characterized by progressive development of fluid- filled biliary epithelial cysts throughout all segment of the liver . **(Dr yuranga et al 2016)**

#### **2-4-1-2 Infectious inflammatory conditions**

##### **2-4-1-2 -1 Hepatic abscesses**

Hepatic abscesses like abscess elsewhere, are localized collection of necrotic, inflammatory tissue caused by bacterial parasitic or fungal agents .bacterial abscesses are most common, usually in the setting of co-morbidity sych as:

Infection elsewhere (most common), abdominal sepsis (most common), necrotizing enter colitis (portal venous drainage), and immune compromised (diabetes mellitus, HIV/ AIDS, elderly, malignancy, and trauma.

Parasitic abscess in patients include

Amoebae (amoebic hepatic abscess), echinococcal (hydrated disease of the liver), protozoa, and helminths.

Ultrasound appearance as general rule: bacterial and fungal abscesses where as amoebic abscesses are more frequently common in a sub-diaphragmatic location and they are more likely to spread through the diaphragm and into the chest. When infection spread to the liver through the portal veins it arises more commonly in the right liver lobe, probably due to an unequal distribution of superior and inferior mesenteric vein contents within portal venous distribution.

Liver abscesses are typically poorly demarcated with a variable appearance, ranging from predominantly hypoechoic (still with some internal echoes however) to hyperechoic. Gas bubbles may also be seen. Color Doppler will demonstrate absence of central perfusion. (Aprof frank, et al 2016)

Amoebic hepatic abscess

Amoebic hepatic abscesses are a form of hepatic abscess resulting from *Entamoeba histolytica* infection. They tend to be rounded or oval and be variable in size although most are round 2.5 cm in diameter; an enhancing wall is present in most cases. The margin of the abscess tends to be smooth in around 60% of cases and nodular in around 40%. Internal septation may be present in around 30% of cases. Focal intrahepatic biliary duct dilatation peripheral to an abscess may be uncommon present

On ultrasound usually appear as hyperechoic lesion with low level internal echoes and absence of significant wall echoes. (Dr Yuranga et al 2016)

#### **2-4-1-2 -2 Hepatic hydrated cyst:**

Hepatic hydrated disease is a parasitic zoonosis caused by *Echinococcus* tapeworm in the liver, two agents are recognized as causing disease in the human, *Echinococcus granulosus* and *Echinococcus multilocularis*. It typically forms spherical, fibrous rimmed cyst with little if any surrounding host reaction



.classically it is a large parent cyst within which numerous peripheral daughter cysts are present. Satellite daughter cysts (outside the parent cysts) are seen frequently. There are two forms of E- granulosus:

Pastoral which is most common form, dog is the main host. The other is sylvatic, which the wolf or dog is a main host

On ultrasound hepatic hydrated cyst appears as multi septate cyst with daughter cysts and echogenic material between cysts. Appearance can vary, may show a double echogenic shadow due to a per cyst. (**Aprof Frank et al 2017**)

### **Hepatic alveolar Echinococcus (HAE):**

It is a rare case of hepatic hydrated disease caused by Echinococcus multilocularis. It is mimic slow growing tumors as in contrast to e granulosus it does not form a well encapsulated mass .but rather infiltrate the liver and its surrounding structures especially at porta hepatis (hepatic veins, inferior vena cava, and biliary tree).

It is usually presents as a large (10 cm) multi loculated/confluent necrotic mass without a fibrous capsule .it has irregular margins with nodular components ,but does not demonstrate central enhancement , up to 385 of cases have peripheral liver reaction enhancement .(**Aprof Frank et al 2017**)

## **2-4-1-3 Neoplastic cystic tumors**

### **2-4-1-3-1 biliary cyst adenoma**

Biliary cyst adenomas , are uncommon benign cystic neoplasm of the liver ,it occur predominantly in middle aged patients and more common in women .biliary cyst adenomas are cystic neoplasm that maybe either unilocular or multilocular ,only rarely are they found in the extra hepatic biliary and gallbladder. Histologically, cyst adenomas are composed of multiple cysts lined by cuboidal or columnar epithelium that a resemble normal biliary epithelium. Biliary cyst adenomas range in size from 3 to 4 cm.

On ultrasound biliary cyst adenomas appear as unilocular or multilocular cysts with enhanced through transmission. The content of the cyst may from completely an echoic to having low-level echoes from blood products much or more protienaceous fluid. Mural nodules and papillary projections may project into cyst lumen .if septal or wall classification is present the a caustic shadowing maybe seen. **(Radswiki et al 2017)**

#### **2-4-1-3-2 Biliary cyst adenocarcinomas**

Biliary cyst adenocarcinomas are a rare cystic hepatic neoplasm. They can be through or a malignant counter part of biliary cyst adenomas. There is recognized increased female predilection .its incidence peak is around 60 years of age. The vast majority of these neoplasms are intra hepatic (97%) with a small proportion extra hepatic (3%).Some cyst adenomas may rarely develop into cyst adenocarcinomas. They typically have seen as a single multilocular cystic tumor with septal or mural nodules.

Imaging cannot reliably differentiate cyst adenoma from cyst adenocarcinomas, but the presence of septal modularity may favour the diagnosis of biliary cyst adenocarcinomas versus a biliary cyst adenoma. . **(Dr Yuranga et al 2017)**

#### **2-4-1-3 -3 Cystic hepatic metastases**

Cystic hepatic metastases are included in the differential for new cystic liver lesions. the internal component may represent necrosis as the tumour outgrows its hepatic blood supply or it may present a mucous component , similar to the primary tumor. The liver and lungs are the most common site of metastases. Cystic hepatic metastases may arise from any number of primary tumours,but classically hepatic metastases arise from organs that have the opportunity of seeding the liver with metastases via portal vein ,including gastrointestinal tract (stomach, small bowel , colon )and pancreas. The appearance of metastases will vary depending on the primary . multiplicity is a classic features of hepatic metastases .

On ultrasound target lesions and hyper echoic lesions are more common appearances for hepatic metastases than cystic lesions : centrally hypo echoic, may have thick septation , hypo echoic halo corresponding with proliferating metastatic cells or compressed hepatic parenchyma , and may demonstrate increased vascularity on Doppler imaging . **(Dr Matt, et al) 2016**

#### **2-4-2 Hyper vascular liver legions:**

Hyper vascular liver legions maybe caused by primary liver pathology or metastatic disease.

The primary liver lesions: such as hepatocellular carcinoma haemangioma, focal nodular hyperplasia, hepatic adenoma, and primary hepatic characinoid.

Metastases from certain primaries demonstrate increase in number of vessels, resulting in a hyper echoic appearance in ultrasound these primary typically include renal cell carcinoma (RCC), thyroid cancer, Leo mayo sarcoma, neuro endocrine tumors, melanoma, and breast cancer , **.(Aprof Frank et al 2016)**

#### **2-4-3 Liver tumors:**

Liver tumors like tumors of any organ can be classified as primary or secondary metastases, which include metastases, primary malignant and primary benign

##### **2-4-3-1 Secondary malignant liver lesions**

###### **2-4-3-1-1 Metastases (Mets)**

Liver metastases are by far the most common hepatic malignancy , with many of the most common primaries readily seeding to the liver. This is especially the case with gastro intestinal tract tumours, but to portal drainage through the liver .the most common sites of primary malignancy that metastasize to the liver are :

Gastrointestinal tract (via portal circulation) which include: colorectal carcinoma, pancreatic ductal adenocarcinomas. Esophageal carcinoma, gastric carcinoma, gastrointestinal tumors, and breast cancer.

Genitor urinary system which include ovarian cancer, endometrial cancer ,and renal cell carcinoma

On ultrasound in general however metastases may appear as : rounded and well defined , positive mass effect with distortion of adjacent vessels, hypo echoic most common 65% and is a concerning feature , hypo echoic halo due to compressed and fat spread liver , and cystic ,calcified infiltrative and echogenic appearance are all possible. (**Aprof Frank et al 2016**)

### **2-4-3-2 Primary malignant tumors**

#### **2-4-3-2 -1Hepatocellular carcinoma ( HCC)**

Is the common primary malignancy of the liver .it is strongly associated with cirrhosis from both alcohol viral dialogue . HCC is the third most common cause of cancer related death.

The origin of HCC is believed to related to repeated cycles of necrosis and regeneration irrespective of cause. On gross pathology, HCC typically appear as pale masses within the liver, and maybe unifocal or multifocal or diffusely infiltrative. Microscopically they range from well differentiated to undifferentiated The macroscopic growth of HCC is usually categorized into three subtypes, nodular, massive, and infiltrative.

On ultrasound the variable appearance depending on the individual lesion size, and echogenicity or background liver . Typically: small focal HCC appears hypo echoic compared with normal liver. Large lesions are heterogeneous due to fibrosis, fatty changes, necrosis and calcification. A peripheral halo of hypo echo genicity may be seen with focal fatty sparing. Diffuse HCC may be difficult to identify from background cirrhosis. ( **Aprof Frank et al 2016**)

#### **2-4-3-2 -2Cholangiocarcinoma:**

Cholangio carcinoma is a malignant tumor arising from cholangiocytes in the biliary tree. It is the second most common primary hepatic tumors, it can be either

intra or extra hepatic. Intrahepatic exophytic nodular (peripheral) tumors are the most commonly of the mass-forming type .They demonstrate variable amounts of central fibrosis, usually marked. On ultrasound the tumors will be heterogeneous mass of intermediate echogenicity with a peripheral hypo echoic halo of compressed liver . they tend to be well delineated but irregular in outline and are often associated with capsular reaction. (**Aprof Frank et al 2016**)

#### **2-4-3-2-3 Primary lymphoma:**

primary hepatic lymphoma (PHL) is primarily found in immune compromised patients such as AID/HIV , Congenital immunodeficiency, immune suppress and therapy for organ transplant .

Primary liver lymphoma are diffuse large B-cell lymphoma other historic types include peripheral T-cell leukemia

On ultrasound

typically hypo echoic to the liver parenchyma probably due to high cellularity and lack of background stroma.

Rarely they may be hypo echoic that they appear similar to a cyst . Occasionally they have a target appearance with a central hyper echogenicity and outer hypoechogenicity .the increased peripheral vascularity on Doppler appear ( **Dr Yuranga etal 2017**)

#### **2-4-3-2-4 Hepatoblastoma:**

Is the most primary malignant tumor in children under four year of age. It is a tumor of embryonic origin. Macroscopically hepatoblastoma are usually relatively well circumscribed large masses, usually single with heterogeneous cut surface.

On ultrasound, hepatoblastoma appear as predominantly soft tissue mass, in large tumor heterogeneity and variable echogenicity is common. Even when large they tend to be relatively well defined .intralesional calcifications maybe visible as areas of shadowing. (**Aprof Frank et al ) 2016**

### **2-4-3--3 Primary benign liver tumors**

Haemangioma, biliary hamartoma, hepatic adenoma and focal nodular hyperplasia.

#### **2-4-3-3-1 Haemangioma:**

Hepatic haemangiomas also known as hepatic venous malformation they are non Neoplastic liver lesions .they are much more common in female .they are thought to be congenital in origin , no Neoplastic and almost always of the cavernous subtype as typical blood supply is predominantly hepatic arterial similar to other tumours ,peripheral location within the liver is most common and atypical hepatic haemangioma .

On ultrasound hepatic haemangioma appear as typically well-defined hyperechoic lesions, a small proportion (10%) are hypo echoic which may be due to a background of hepatic steatosis , where the liver parenchyma itself is of increased echogenicity . may show peripheral feeding vessels in colour Doppler .(Dr Yuranga et al 2016)

#### **2-4-3-3-2 Hepatic adenoma:**

Hepatic adenoma is an uncommon benign liver tumor that is hormone induced.

The tumours are usually solitary and have predilection to hemorrhage and large (5-15 cm)from other focal liver lesions. it is most frequent hepatic tumor in a young women who are on oral contraceptive pill. Hepatic adenomas are most frequently seen at a sub capsular location in the right lobe of the liver and are often a round.

Well defined pseudo encapsulated mass, occasionally dystrophic calcification may be present. Multiple lesions are frequently observed in patient with type1 glycogen storage disease

On ultrasound hepatic adenoma usually presents as solitary well demarcated heterogeneous mass. Echogenicity is variable: hypo echoic 20%-40%, hyperechoic up to 30%

Hypo echoic halo of focal fatty sparing is also frequent seen .maybe show perilesional sinusoids on color Doppler .( **Dr Kosky et al2016**)

### **2-4-3--3 -3 Focal nodular hyper plasia:**

Focal nodular hyperplasia (FNH) is a benign tumor - like mass of the liver second only to cavernous haemangioma in frequency. Focal nodular hyperplasia is most frequently found in young to middle –aged adult with a strong female predilection. The origin of FNH is thought to be due to hyper plastic growth of normal hepatocytes with a malformed biliary drainage system. it is also believed to be in response to a pre- existent arterio-venous malformation .focal nodular hyperplasia divided into two types typical and atypical .

Typical : demonstrate a tumor which is often quite large with well- circumscribed margins but poorly encapsulated ,with prominent central scar , radiating fibrous septate .

Atypical: refer to lesion which lacks the central scar and central artery .atypicall features also include pseudo capsules lesion heterogeneity.

On ultrasound the echogenicity of both FNH and its scar is variable and it maybe difficult to detect on ultrasound .soma lesions are well marginated and easily seen where other are iso echoic with surrounding liver. Detectable lesions characteristically will demonstrate a central scar with the displacement of peripheral vasculature on colour Doppler.( **Aprof Frank et al 2016**)

## **2-5 Ultrasound Examination technique:**

### **2-5-1 Patient Preparation:**

It is recommended that a patient undergo a period of fasting prior to upper abdominal imaging to maximize the distension of the gall bladder and to reduce food residue and gas in the upper GI tract which may reduce image quality or precluded liver imaging. This is essential for full imaging of the liver and related

biliary tree but may not be required in an acute situation such as trauma where imaging of the gall bladder is not immediately essential. A patient may take small amounts of still water by mouth prior to scan, particularly for taking any medications. There is some evidence that smoking can reduce image quality when scanning upper abdominal structures and it is good practice to encourage a patient not to smoke for 6-8 hours prior to US scan. Smoking increases gas intake into upper GI tract and may reduce image quality. Also, some chemicals in tobacco are known to cause contraction of the smooth muscle of the GI tract and this can cause contraction of the gall bladder, even when fasting has occurred, and the gall bladder cannot be scanned. **(Christoph, 2004)**

### **2-5-2 Son graphic technique:**

TAUS usually begins with the patient in the supine position. The examiner is on the patient's right side and the ultrasound machine is on the same side toward the head of the bed. A 3.5 MHz curvilinear transducer is the most common one used in adults. The curvilinear transducer requires a larger, flatter surface for optimal contact. When a smaller "footprint" (size of the contact surface) is necessary, such as viewing through an intercostal space, a phased array transducer can be used. Ideally, prior to TAUS, the patient should fast for 6 h. This decreases bowel gas and allows gallbladder distension. Standard scanning planes for TAUS are: longitudinal (sagittal, coronal) and transverse. Most TAUS scanning is done with light contact with coupling accomplished with gel. When holding the transducer, it is helpful to stabilize your hand by placing the base of the hypothenar eminence against the body. This allows for fine probe movement during the examination. The initial transducer placement depends on the type of study or organ of interest. The same is true for the initial transducer orientation. Transducer movement during TAUS includes all the techniques previously described. **(Ellen, 2014)**



The patient should be examined from the sub- to the intercostal in the decubitus position as well in the modified, slightly oblique, positions with the right arm above the head and the right leg stretched during all respiration cycles to identify the best approach and to avoid artifacts caused by the thorax. Examination in the standing position is also helpful owing to the liver moving caudally with gravity. Scanning from the sub- or intercostal probe positions (depending on the individual anatomy) avoids interposed lung, which can occur in the right posterolateral (superficial) parts of the liver when using the intercostal approach. There are other examination techniques that can also be used, but these will not be mentioned here in detail (Jan 2013). One measurement of liver size is done in the mid-clavicular line from highest peak of the diaphragm down to the caudal liver end. This has a maximum dimension 18 cm. Another possibility to measure the liver size is in the mid-clavicular line to measure ventrodorsal dimension (depth) and cranio-caudal dimension (length). The maximum length is 15 cm and depth 13 cm, maximum for both dimensions together is 28 cm. In many diseases, the caudate lobe is larger than the rest. In the liver cross section, measurement of this lobe relative to the rest, the quotient should be normally less than 0.55. **(Jan Tuma, 2013)**

## **2-6 Previous studies:**

Many studies were published regarding to characterization of benign and malignant liver lesions by ultrasound and texture analysis several methods have been proposed for diagnosis and classification of liver lesions .most of these studies done locally and internationally by many researchers.

Millat et al (2011) studied the neural net work based focal liver lesion diagnosis . They proposed a computer-aided diagnostic system aimed to assist radiologist in identifying focal liver lesions in b-mode ultrasound images. The proposed system can be used to discriminate focal liver disease such as cyst, haemangioma, hepatocellular carcinoma , and metastases, along with normal liver.thet performed

with 111 real ultrasound images comprising of 65 typical images, and 46 atypical images, which were taken from 88 subjects. These images were first enhanced and then region of interest are segmented into 800 non-overlapping segmented region of interest. By using a new methodology which handles simultaneously on enhancement and speckle-reduction process, subsequently 208 texture based features were extracted from each segmented region of interest using statistical, spectral and TEM methods to feed a two-step neural network classifier. They recorded classification accuracy of 86%. The classifier has given correct diagnosis of 90.3% (308/340) in the tested segmented region of interest from typical cases and 77.5% (124/160) in tested region of interest from atypical cases. They employed traditional methods (e.g. ANNs) which aimed to minimize the empirical training errors.

Vermeni et al (2013) proposed a computer-aided diagnostic system (CAD) for focal liver lesions based on texture inside and outside the region in classification of focal liver lesions (FLLs). They collected the database from 108 B-mode ultrasound images from the patients visited the Department of Radio diagnosis and imaging Post Graduate Institute of Medical Education and Research, Gandharh India over the time period from March 2010 to March 2012. These images comprised of 21 Normal images, 12 Cyst images, 15 Haemangiomas lesions, 28 HCC lesion images, and 23 Mets lesions. Texture features were computed from inside and outside of the region of the lesions, two type of features were considered for analysis, i.e. texture features and texture ratio features. Features set consisted of 208 texture features. Principal Component Analysis (P.C.A) was used for finding the optimum number of principal components to train SVM (support vector machine) classifier for the classification task. Their proposed PCA-SVM based CAD system yielded classification accuracy of 87.2%, with the individual class accuracy of 85%

,96%,90%,87.5%,and 82.2%of NOR ( normal), Cyst, HEM (Hemangioma), HCC (Hepatocellular carcinoma),and MET( Metastases) cases respectively using ten fold cross validation .However, this system does not have image preprocessing and image segmentation components. in such system only some texture features obtained directly from the images or ROIs (Region of interests)one used as inputs of the classifiers. That the feature extracted directly from ROIs may not provide robust and accurate performance.

Yoo Na Hwang et al (2015)classified focal liver lesions on ultrasound images by extracting hybrid textural features and using an artificial neural network they focused on the improvement of the diagnostic accuracy of focal liver lesions by quantifying the key features of cysts, haemangiomas, and malignant lesions on ultrasound images . their study performed with 115 patients presented with 99 focal live lesions, which divided into 29 cysts,37 haemangiomas, and 33malignancies . they obtained all images with an Acuson Sequoia 512 ultrasound imager ,the resolution for the gray level image was 640x480 pixels. The training frequency of the ultrasound was set to 20 MHz and the receiving harmonic bandwidth was 4.0 MHz the specific characteristic of each lesion were obtained by selecting a Region of interest(ROI) OF 52X52 pixels -122X157 pixels from the original image. A total of 42 hybrid textural features that composed of 5 first order statistics,18 gray level co-occurrence matrices , 18 laws , and echogenicity were extracted .A total of 29 key features that were selected by principal component analysis were used as asset of input for a seed-forward neural network .for each lesion, also the performance of the diagnosis was evaluated by using the positive predictive value, negative predictive value, sensitivity, specificity ,and accuracy. The result of experiment indicate that the proposed methods exhibits great performance , a high diagnosis accuracy of over 96% among all focal liver lesion

groups (cyst vs. haemangioma, cyst vs. malignant, and haemangioma vs. malignant) on ultrasound images. They concluded that the accuracy was slightly increased when echogenicity was included in the optimal feature set, and indicate that it is possible for the proposed method to be applied clinically .

Jetendrae et al. (2013) studied characterization of primary and malignant liver lesions from B-mode ultrasound. they collected their data from 51 different patients with 51 images (out of these 27 images were HCC images with 27 solitary HCC lesions and 24 images were MET images with 27met lesions, I.e.21met images with solitary met lesion and 3 met images with 2 met lesions each. The direct digital images recorded by using Philips ALT HDI 5000ultrasound machine equipped with multi frequency transducer of 2-5MHzrange. The size of images was 800x 564 pixels with gray scale consisting of 256 tones ,and horizontal as well as vertical resolution is 96 dpi . they investigated the contribution made by texture patterns of region inside and outside of the lesions for binary classification between HCC and MET lesions. They performed on 51 real ultrasound liver images with 54 malignant lesions i.e. 27 images with (27 solitary HCCs , 13 small HCCs and 14 large HCCs) and 24 images with 27mets lesions(12 typical cases and 15 atypical cases).A total of 120 within-lesion region of interest and 54surrounding lesion region of interest were cropped from 54 lesions subsequently, 112 texture features (56 texture features and 56 texture ratio features)were computed by statistical, spectral ,and spatial filtering based texture features extraction methods .they used two-step methodology for feature set optimization i.e. feature pruning by removal of nondiscriminatory features followed by feature selection by genetic algorithm-support vector machine (SVM) approach which designed based on optimum features .they found that the ratio features were more discriminatory than WLROI features for characterization of

HCC and MET focal liver lesions . only nine texture features (seven ratio feature and two WLROI features) were significant to account for textural variations exhibited by HCC and MET lesion. They concluded that the texture of background liver on which the lesion had evolved did contribute towards characterization of primary and secondary malignant liver lesions from B-mode ultrasound. The proposed computer-aided diagnostic system achieved the overall classification accuracy of 91.6% with sensitivity of 90% and 93.3% for HCCs and METs cases respectively. Finally their results indicate that the proposed CAD system can be routinely used in a clinical environment to assist radiologist in diagnosing liver malignancies and there be facilitate in providing better disease management.

Delia et al. (2012) studied the role of superior order GLCM in the characterization and recognition of the liver tumors from ultrasound images aimed to develop computerized ,non invasive techniques for the automatic diagnosis of HCC based on information obtained from ultrasound images, also they determined the best spatial relations between the pixels that lead to the highest performances, for the third , fifth ,and seventh order GLCM .Their dataset contained the classes of HCC, Cirrhotic liver parenchyma on which HCC evolves and benign liver tumors. They formed the dataset from 300 cases of HCC and 150 cases of benign tumors of the following type: haemangioma, hepatocellular adenoma, focal nodular hyperplasia . they considered three image for each patient, the ultrasound images were acquired using various orientation of transducer ,under the same setting of the logic 7 ultrasound machine ,the frequency was 5.5MHz,the gain was 78 dB ,and the depth was 16cm . each class was formed by region of interest selected on desired type of tissue. the classes were combined in equal proportion. they discriminated HCC from the cirrhotic liver parenchyma on which it evolves using the third order GLOM. They performed the selection of the relevant textural features using the methods of correlation-based feature selection (CFS),respectively

of Gain Ratio Attribute Evaluation, after applying the third order GLCM for each considered pair of directions separately.

They also discriminated HCC from the benign liver tumors by obtained support vector machines (SVM) and using both the second and seventh order textural features ,in combination with the other old textural features . they obtained the result that in the case of the second order GLCM, the average value of the maximum probability was 0.05 , for the third order (GLCM) this value was 0.01, for the fifth order (GLCM) this value was 0.0005. they noticed that the value of maximum probability had in the case of HCC was lower values than that in the case of cirrhotic parenchyma and of the benign tumors due to irregular, chaotic character of the malignant tumors .for the HCC tumor, group of pixels having hypoechogenic values appeared frequently .

They concluded that the textural features proved to be appropriate for the characterization and recognition of HCC. the superior order GLCM features lead to recognition rate situated above 81%.the group of specific gray- level values met the most frequently inside the tumors corresponded to the structural component of this kind of tissues.

Dalwali et al (2013) studied an automatic boundary detection and generation of region of interest for focal liver lesion ultrasound image using texture analysis. they proposed an automatic ROI generation for focal liver lesion ultrasound images .Firstly, some techniques of speckle noise reduction would implemented consist of ,median,mean,Gaussian low-pass and wiener filter. Then texture analysis was performed by calculated the local entropy of the image, continued with the threshold selection, morphological operations, object windowing, seed point determination and region of interest generation .They used TOSHIBA APLIO X ultrasound machine with 3,5MHz transducer. MATLAB (MATRIX

LABORATORY) programming which followed by algorithm was used to developed the system for generating the focal liver lesion ultrasound region of interest automatically .they used the gradient vector flow (GVF ) speckle noise model for automatic boundary detection and GLCM ( Gray Level Co- occurrence Matrix ) methods for texture analysis .the computation of texture features was done through specific texture analysis methods . the first order statistics of gray level ,GLCM Fractal,-based method, and transformed –based methods. Their result showed that the images were blurred compared to the original image, after applied speckle noise reduction techniques which are median filter, mean filter, wiener filter and gaussian low pass filter .they saw that all those output images were used for region of interest generation to compare which filter gives the best output .gaussian low pass filter images gave better result for boundary detection of region of interest. They concluded that for focal liver lesions us images, texture analysis by using GLCM feature extraction methods better compared to range and standard deviation filter .based on comparison between speckle noise reduction techniques, median filter gave the highest true ROI which were 100% after being tested using threshold value 0.7.the generation of true ROI can be used as a preprocessing methods for any other segmentation techniques. This ROI generation can make next image processing method is faster.

Hiral etal (2014) studied ultrasound evaluation of focal liver lesions aimed to evaluate the role of ultrasound in evaluation of focal liver lesion , to study the imaging spectrum of focal hepatic lesions and to correlate the ultrasound finding with FNAC and/ or CT scan. Their study done at the department of radiology PDV GOVT. Medical College and Civil Hospital Rajkot, Gujerat. India. Their study comprise of 50 patients diagnosed by ultrasound, most of focal liver lesions were abscess, haemangioma, cysts, metastases, primary liver tumors, and hydated cysts.

They used Philips IU22 . convex (1-5MHz), linear(3-9 MHz),linear(5-17 MHz) transducer used. Their result showed that the ultrasound had an average specificity of 93.6% with 100%specificity for common benign lesions like haemangioma and cyst. They concluded that the ultrasound is highly sensitive in diagnosing focal liver lesions such as abscess, metastases, and primary malignant liver tumors and hydrated lesions. With specificity of 94.4%, 85.7%, 75and 100% respectively . The great majority of asymptomatic single lesions were being hepatic cyst and haemangiomas with classic appearance can be safely diagnosed with ultrasound alone. They evaluated that the ultrasound had a wide applicability, being a safe, simple, repeatable, so it is worthy of being included in routine diagnostic work also they concluded that there is a significant association between ultrasonography and finding and FNAC diagnosis.

Jetendra etal (2014) proposed a neural network ensemble based computer-aided diagnostic system (CAD) for focal liver lesions from B-Mode ultrasound to assist radiologist in differential diagnosis between focal liver lesions including typical and atypical cases of cyst, haemangioma, metastatic carcinoma lesions, small and large hepatocellular carcinoma lesions along with normal liver tissues. A total of 108 b-mode liver ultrasound images were collected from the patients visited the department of radio diagnostic and imaging at post graduate institute of medical education and research (Chandigarh India) they used to record images Philips ATLHHDI 5000 ultrasound machine with multi-frequency transducers .They collected the data by an experience radiologist ensured that all images were of diagnostic quality (free from artifact)and confirmed the presence of Cyst, HEM, HCC , and MET lesions . They consider only HCC evolving cirrhotic liver . their selection of region of interest (ROIs) by cropped it from database by an experience participating radiologist by using aspecially designed ROI manager



software developed in biomedical instrumentation Laboratory, Indian Institute of Technology Roorkee. They choose the ROI size and shape, move the ROI at any desired location over the image, freeze the ROI at any location and crop the ROIs together after the position of all the ROIs for a particular image is frozen. They used two types of ROIs: inside ROIs (IROIs) and surrounding ROIs (SROIs). For each cyst, hem, hcc, and met lesion, the maximum non-overlapping IROIs were cropped from well within the boundary of each lesion. For each lesion, a single SROI was cropped from surrounding liver parenchyma approximately at the same depth as that of the center of the lesion by avoiding the inhomogeneous structures like liver ducts and blood vessels. For each NOR image, a single extreme ROI was considered as SROI, and all other ROIs at the same depth were considered as IROIs. SROIs and IROIs for NOR image were cropped by avoiding the inhomogeneous structures like liver ducts and blood vessels. They visualized the textural characteristics of region inside and outside the lesion to differentiate between different FLLs, accordingly texture features computed from inside lesion region of interest (IROIs) and texture ratio features computed from IROIs and surrounding lesion region of interest (SROIs) were taken as input. They used principal component analysis (PCA) for reducing the dimensionality of feature space before classifier design. They incorporated two steps of classification modules: the first one consists of a five-class PCA-NN based primary classifier which yields probability outputs for five liver image classes. The second step of classification module consists of ten binary PCA-NN based secondary classifiers for Nor/Cyst, Nor/Hem, NOR/Hcc, Nor/Met, Cyst/Hem, Cyst/Hcc, Cyst/MET, Hem/Cyst, Hem/Met, and Hcc/Met classes. The probability outputs of five-class PCA-NN based primary classifier were used to determine the first two most probable classes for a test instance based on which it is directed to the corresponding binary PCA-NN based secondary classifier for crisp classification.

between two classes. By including the second step of the classification module, classification accuracy increase from 88.7% to 95%.the promising results indicate that the proposed NNE based CAD system can be routinely used in clinical environment to assist the radiologist in lesion interpretation and differential diagnosis of focal liver lesions using conventional B-Mode gray scale ultrasound images .

Ulagamuthalvi (2012) proposed an automatic identification of ultrasound liver cancer tumor using support vector machine aimed to design a diagnostic classifier system for identifying liver tumor in ultrasound images using texture features in anon- I invasive manner .they applied the co-occurrence matrix features and gray level run -length features for identifying the seed point for given ultrasound liver images. and then they had to segmented the liver image by applying thr region growing algorithm using gray space map and OTSU allogrith . After segmentation of the image they analyzed calculated texture features parameters to classified, as normal benign and malignant liver tumors. Their result showed that the support vector machine which used as a classifier offers the better result in identifying the malignant liver tumor from the normal. The overall accuracy of classification value 97. 72% approximately for the ultrasound liver images .

Alietal(2014) proposed an automated identification and classification of various stages of focal liver lesions based on the mult-support vector machine (Multi S.V.M). which used to discriminate focal liver disease such as cyst, haemangioma. Hepatocelular carcinoma along with normal liver. They applied Multi s,v,m to classify the diseases using haralich local texture descriptors and histogram based feature calculated from region of interest (ROI) as input which selected automatically by using Fuzzy c-mean initialized by level set technique. they Adopted the one against all (OAA) method for multi class classifications. They

collected 150 different liver disease picture ,they had chosen 94with best quality and best applicability in pattern recognition area. those images represented three different focal liver lesion disease cyst haemangioma and hepatocellular carcinoma, they enhanced the image by using anew methodology called spatial filter. and remove noisy from the images , the segmentation of region of interest was done in an automatic way with the aid of fuzzy c-mean and level set technique which assist to extract contours of liver tumors from ultrasound images with a very high reliability. they analyzed and extracted Haralich and histogram based features from the suspicious area and region of interest(ROI). In their work a total of 94 features had been extracted from each region of interest of liver ultrasound images ,namely 6 histogram features and 88 GLCM based texture features. they had measured those features from ROI for every image of three categories along with normal. after dimensionality reduction using rough sets they obtained 38 features which were used to train and test the Multi svm classifier. They given 4 classes, 4 independent binary svm classifiers were constructed where the first classifier discriminates primary cyst from haemangioma ,hepatocellular carcinoma and normal liver, the second discriminates haemangioma from cyst, hepatocellular carcinoma and normal liver, the third discriminates hepatocellular carcinoma from cyst ,haemangioma and normal liver and the fourth discriminates normal liver from cyst, haemangioma and hepatocellular carcinoma. They had obtained 96.11% with the individual class accuracy of 97.78% ,95.56% ,93.33% and 97.78% for NOR,CYST,HAEM and HCC cases respectively .they concluded that it is usefull to discriminate between focal liver diseases such as cyst, haemangioma and hepatocellular carcinoma along with normal liver. finally they demonstrated that the good performance of the proposed method showed a reliable indicator that can improve the information in the staging of focal liver lesion diseases .

Poonguzhali et al. (2008) studied an automatic classification of focal lesion in ultrasound liver images using combined texture features, aimed to build a computer-aided automatic early detection system for the identification of cyst tumors and cancers by analyzing unique echotexture patterns using a custom designed back propagation neural network classifier. The images were collected from hospital on various patients taken with ALT HDI 5000 ultrasound machine using curvilinear and sector array of frequency 4 MHz under similar imaging conditions. They extracted texture features using various statistical and spectral methods. They preferred four selection methods for texture description: Gray level co-occurrence matrix based statistical texture features e.g. the second order image histogram, Gray level run length matrix based statistical texture feature, low-pass spectral texture feature, and Gabor Wavelet-based spectral texture features. The combined features were used to classify those images into four classes: normal, cyst, benign and malignant masses. The images of each class were collected and 30 sub images from each class were used as the image database. Their results showed that the performance of the classifier is good for cyst since they are most homogeneous texture and distinct among the four classes. Also this classifier offers better results in identifying the malignant lesion from the surrounding normal region. They misclassified the benign tumors as normal in some cases as their texture were quite similar, the shape and symptoms help the doctors easily differentiate the benign tumors from the normal parenchyma. The overall accuracy of the images is nearly 83% for the liver images in their database. They concluded that a multi-class multi-variant problem like classification of the focal lesions of the liver using ultrasound liver images was automated by the selection of optimal features and back propagation network. The initial implementations of the combined texture vector for classifying the liver lesion were promising as it yields better rate of classifications.

Vishwanat(2013) evaluated focal liver lesion by ultrasound as a prime image modality ,he aimed to diagnose different types of focal liver lesions by ultrasound and to assess the validity of ultrasonographic diagnosis in relationship to FNAC diagnosis. His study comprised of 105 cases of focal liver lesion studied by ultrasound for a period of one year conducted in the department of radiology and later the finding confirmed by FNAC,his result showed that males had increased in predilection than females, liver abscess, primary malignant liver tumors, and metastases had highest incidence in the age group of 41- 50 years with 14-15-10 cases respectively, and the majority of liver lesion were involved the right lobe in 64.8%of cases and solitary in 61.9%of cases. He concluded that ultrasonography is highly sensitive in diagnosing focal liver lesions such as liver abscess, primary malignant liver tumors, and metastases which constituted the majority of focal liver lesions with sensitivity of 90.9%,80.6%,and 76.9% respectively. And also concluded that ultrasonography had a wide applicability in the diagnosis of focal liver lesions ,being safe ,simple, repeatable, and without radiation exposure to the patients. It is worthy included in routine diagnostic work due its highly sensitivity and specificity of diagnosing focal liver lesions.

Ulagamuthalvi and Sridharan(2012) focused on development of diagnostic classifier for ultrasound liver lesion images, they prepared the ultrasound liver image for further processing such as segmentation and classification by reducing the speckle noise with getting a high –pass filter, after removing the noise from the image they applied co-occurrencematrix and gray level run- length features for identifying the seed point for given ultrasound liver images, after the detection of automatic seed point ,they had to segment the liver image applying the region growing algorithm using gray space map and OTSU algorithm , then they

analyzed and calculated textural features parameters to classified as normal ,benign and malignant liver lesions. They used support vector machine( SVM) classifier based on the risk bounds of statistical learning theory .The textural features for different feature methods were given as input to the SVM individually . Performance analysis train and test dataset carried out separately using SVM Model. Whenever an ultrasound liver lesion image was given to the SVM classifier system ,the features were calculated ,classified as normal ,benign and malignant liver lesions. they resulted that the SVM classifier offers the better result in identifying the malignant liver tumor from the normal. In some case4s the benign tumor were misclassified as normal liver and benign maybe same. the overall accuracy of classification value 96.72% approximately for the ultrasound liver images. So they conducted that this system will help the physician to diagnose the liver lesion with noninvasive.

Deeptietal (2016) studied detection and classification of focal liver lesions using support vector machine classifier. their study performed to design computer aided diagnostic system to detect and classify focal liver lesions such as cyst , haemangioma, hepatocellular carcinoma and metastases using support vector machine {SVM}classifier by evaluated clinically acquired ultrasound images from88 patients with total of database which contains 111liver ultrasound images comprising 95 images of focal lesions (17 cyst,15HCC,18 HEM, and 45 METS)and 16images of normal liver images. Those images were enhanced by regularized MSRAD-Template 9 methods, and manually segmented into 800 non overlapping segmented region of interest. they used five texture based extraction methods from first ,second and higher border statistics , along with spatial filtering and multi- resolutional approached to achieve good classification accuracy .the method chosen were first order statistics ,spatial gray level dependence matrix,

gray level run-length matrix, texture energy measures and Gabor wavelets respectively. They extracted 208 textural features from each segmented region of interest. First diagnostic system was designed with one-against-one multi class support vector machine classification approach showed 93.01% {512/550} overall accuracy on test dataset. Second diagnostic system was designed with tree structured approach using four binary support vector machine classifier showed 86.9% {487/550} overall accuracy on datasets. They concluded that SVM-CAD system with tree structured approach can produce high accuracy rate 86.9% in focal liver lesion detection and classification. The approach is a valuable to improve the accuracy of the diagnosis of liver cancer and to reduce the number of biopsies. CAD system with OAO approach based multi-class SVM classification provides the better results in term of overall accuracy of 93.1% with the selected set of 208 sensitive features. Out of these two, OAO approach based diagnostic system, outperforms the neural network based diagnostic system designed for the same purpose by providing 96.6 % classification accuracy for typical cases and 85.3% for atypical cases.

Nimisha et al (2016) studied the application of texture features for classification of primary benign and malignant and primary malignant focal liver lesions. They focused on the aspect of textural variations exhibited by primary benign and primary malignant focal liver lesions by computed these textural variations using statistical methods, signal processing based methods, and transform domain methods. They proposed an efficient CAD system for primary benign (haemangioma) and primary malignant (hepatocellular carcinoma) on textural features derived from b-mode ultrasound images. They computed those textural features from inside region of interest (IROIs) and one surrounding region of interest (SROIs) for each lesion. They extracted these features by using six

features extraction methods namely, FOS, GLCM, GLRLM, FBS, Gabor, and Laws features. They subjected three textural features vectors to classification by SVM AND SSVM classifier. it is observed that the performance of ssvm based CAD system is better than svm based CAD system with respect on overall classification accuracy ,individual class accuracy for atypical HAEM class, and computational efficiency. they obtained the proposed ssvm based CAD system design indicate it is usefulness to assist radiologists for deferential diagnosis between primary benign and primary malignant liver lesion .

Hyung et al(2009) studied a computer aided image analysis of focal hepatic lesions in ultrasonography to develop a computer aided image analysis (CAIA) algorithm for analyzing ultrasound features of focal hepatic lesions, and to correlate the features value of CAIA with radiologist grading. They evaluated sonographic images of 51 focal hepatic lesions in 47 patients (19 Haemangioma,14 simple cyst or cystic lesion,11 HCC, 6 Mets, and 1 focal fat deposition) they graded all images by using a 3 to 5 point scale in terms of border(roundness, sharpness, and presence of peripheral rims.)texture( echogenicity, homogeneity, and internal artifact),posterior enhancement ,and lesion conspicuity. They extracted the texture and morphological parameters representing radiologist subjective evaluations by using CAIA. They computed the correlation between the radiologist and the CAIA for assessing parameters by means weighted K statistics and spearman correlation test . their result showed that there was a good agreement achieved between CAIA and radiologist for grading: echogenicity (weighted K= 0.675) ,and the presence of hyper or hypo echoic rim (weighted K=0.743).several CAIA derived features representing homogeneity of the lesions showed correlations ,(correlation coefficient  $y=0.603-0.641$ )with radiologist grading ( $p<0.05$ ). for internal artifact  $y=0.469-0.490$ , and posterior enhancement= $(0.516)$ of the cyst, and lesion



conspicuity  $y=(0.410)$ . Affair correlation between radiologist and CAIA was obtained ( $p<0.05$ ) ,however parameters representing lesions border such as sharpness ( $y=0.252-0.299$ ) and roundness ( $y= 0.134-0.163$ ) showed no significant correlation ( $p>0,05$ ). They concluded that a CAIA algorithm was constructed with a good agreement and correlation with human observers in most ultrasound features. In addition, these features should be weighted highly when a computer-aided diagnosis for characterizing focal liver lesions on ultrasound is designed and developed.

Salih et al (2014) at national cancer institute, Gezira University Sudan, studied the ultrasound appearance of hepatic metastases from female breast cancer, aimed to evaluate the appearance of liver metastases on ultrasonography. They studied 108 breast cancer patients diagnosed with liver metastases underwent grayscale ultrasonography of mean age was 44years old (range 27-81)years. diagnosed with liver metastases using gray scale ultrasound, data were analyzed by Microsoft excel 2010 SPSS software they were observed that most of metastases were multiple in 92%of cases, where as a single metastases was observed in the remaining 8%cases their study showed liver metastases from breast cancer were hypo echoic, hyper echoic, mixed, (hypo echoic and hyper echoic), and isochoric signal in 70%,21%,6%,and 35 of cases respectively ,they concluded that ultrasonography improves the detection and characterization of multiple metastases with hypo echoic echo pattern.

Saida(2013) studied assessment of liver abscesses by using ultrasound and ultrasound drainage which was conducted from 2008 to 2013,at a private clinic Khartoum hospital street. She used GE Logic P5 with curvi-linear convex transducer with frequencies between (3-5MHz) and Aloka ultrasound machine

SSD3500 using curvi-linear with frequencies (3-5MHz) transducer, her data her data were analyzed by SPSS software .she resulted that males were affected by abscesses more than females, and right lobe was more affected , she observed that the ultrasound appearance of liver abscesses most likely hypo echoic ,well defined rounded in shape with thick walled. she concluded that liver abscesses is a serious common infectious liver disease in Sudan ,and it is easy to be diagnosed by ultrasound ,also it can be completely aspirated and treated by ultrasound guided drainage.

Sakijan(1988) studied ultrasound finding of liver abscess aimed to determined the sonographic pattern of liver abscesses and also identify any features which helpful for correct diagnoses .he studied one hundred sixty five patients (133males and 32 females) over a period from January 1983to December 1987.he used both Philips sonodiagnost static scanner with a 3.5MHz transducer on 10 patients and Philips SDR1500real time scanner with a 3.5MHz sector transducer on the remaining patients. his result showed that the majority of abscesses (84%)were in the right lobe most abscess were round in shape (83%),and the abscess were most hypo echoic in (59%) followed by mixed in( 28%) while the remaining were echogenic in (11%), and with fluid debris in (2%) He concluded that the presence of round, well-defined, smooth hypo echoic mass.

AAhidjoet al between January 2002 and December 2005, at Maidugari teaching hospital . studied correlation between ultrasound finding and ultrasound guided – fine needle aspiration cytology in the diagnosis of hepatic lesions. Aimed to correlate between ultrasound guided fine needle aspiration cytology and ultrasound alone in the diagnoses of focal hepatic lesions .they used ultrasound 9ATL and Doppler ultrasound machine with 3.5MHz curvilinear transducer. Their study

revealed that more males patients with hepatic lesions than female, their showed that out of 47 patients diagnosed by USSG- FNAC ,37 were malignant, six as suspicious of malignancy ,two as amoebic abscess and one as metastatic and liver cirrhosis. Malignancy was the commonest finding by both ultrasound and USSG-FNAC.They conducted that USSG-FNAC may or may not be superior to ultrasound alone in the diagnosis of hepatic local lesions

## **Chapter three**

### **Material and Method**

#### **3-1 Material**

- Toshiba Xario. Diagnostic Ultrasound System. Model SSA-666A, with 3.5 curve-linear transducer and Sony printer.
- General Electric Ultrasound .Model 2104587 with 3.5curv-linear transducer and Sony printer.

#### **3-2 Design of the study**

This is a prospective, descriptive and analytical study which characterizes benign and malignant liver lesions using ultra sonography and texture analysis.

#### **3-3 Population of the study**

The target population for this research defined to include patient with known case of liver lesion presented during the study period.

#### **3-4 Sample size and type**

The data of this study will be collected from 260 patients known with liver lesion that drawn for ultrasound examination. A sheet was designed for collection of data from the patients and his ultrasound image. This sheet includes patient information and results of gray scale ultrasonography.

#### **3-5 Place and duration of the study**

This study was carried out in Ibsina teaching hospital in Khartoum state, and Osman Abdalwahab private clinic for three years from 2016 to 2019

#### **3-6 Variable of the study**

The data will be collected using the following variables: Site, size, shape, and echogenicity, vascularity of the lesion, age, gender, patient size, and liver echo texture.

#### **3-7 Technique: Imaging protocols**

Trans abdominal U/S scanning

## Patient Preparation

The patient must be fasting eight hour prior the examination with full bladder enough.

### Position of the patient:

The patient should lie supine but may need to be rotated obliquely. The patient should be relaxed, lying comfortably and breathing quietly, lubricates the lower abdomen with coupling agent. Hair any where on the abdomen will trap air bubbles so apply coupling agent generously.

### Scanning technique:

Start with a longitudinal scans from the Xiphoid process and we must be angle the probe sharply to the right for setting the gain, move the probe to the right until the right lateral border of the liver appears clearly in the center of the screen. Then move the probe to the left until the left lateral border of the liver appears clearly in the center of the screen. Adjusted the gain of the image and searched for any lesion and defined it as which it echo texture was hyper echoic, hypo echoic, iso echoic, cystic, or mixed(hypo and hyper), be it singl, two or multiple ,with rounded shape or irregular , the size, site within the liver, and left edge of the liver, Then saving the image.

## **3.8 Methods of data collection**

Using a special data collection sheet (questionnaire), sample of 260 patient with liver lesions includes simple cyst, hydrated cyst ,hepatocelullar carcinoma and liver metastases ,were studied by trans abdominal ultrasound scanning and data was collected using a data collecting sheet which designed to evaluate liver anatomy, size, texture, lesion type, size, shape and echogenicity.

## **3-9 Method of data analysis**

All questionnaires were daily checked for completeness and accuracy by the investigator .Filled questionnaire were coded before entering data into the

computer using Statistical Package for Social Science (SPSS) Statistical analysis was performed using SPSS.

For texture analysis:

The U/S images were stored in a computer disk then viewed by the Radiant, Ant DICOM viewer in computer to selected the images that suit the criteria of research population then uploaded into the computer based software Interactive Data Language (IDL) . The U/S image were read by IDL then the researcher clicks on areas represents the background , normal liver parenchyma(for normal), then for disease patients on liver( cyst, HCC ,Hydated cyst and metastases) in test group images, in these areas, these textural features include : mean ,entropy, and energy. These features were assigned as classification centre .A window of 3×3 pixel were generated and first order textural feature for the classes center were generated. After all images were classified the data concerning the, normal, cyst, HCC, Hydated, cyst and metastases entered into SPSS with its classes to generate a classification score using stepwise linear discriminate analysis; to select the most discriminate features that can be used in the classification of abdominal tissues in U/S images. Where scatter plot using discriminate function were generated as well as classification accuracy and linear discriminate function equations to classify the abdominal tissues into the previous classes without segmentation process for unseen images in routine work.

### **3-10 Ethical approval**

Ethical approval was granted from the hospital and the radiotherapy department as well as consent from the patient will be taken that no patient identification will be disclosed. Consent from radiologist, Verbal consent from the patient to see his ultrasound investigation. Confidentiality and privacy will be considered right to benefit and no harm.

## Chapter four

### Result

This study aimed to characterized the liver lesions using ultrasound and texture analysis, comprises of 260 patients with different types of liver lesions underwent successful abdominal ultrasound for a period of three years conducted in the department of radiology at Ibn Sina teaching hospital and Dr Osman Alwahab private clinic .These patients were subjected for ultrasound evaluation, The followed observation were made as tables and figures:

**Table( 4-1) Gender distribution of liver lesion**

<b>Gender</b>	Frequency	Percent
Female	104	40.0
Male	156	60.0
Total	260	100.0

**Table (4- 2) Age distribution of liver lesions**

Age grouped	Frequency	Percent
4-13.5	4	1.50%
13.6-23.1	2	0.80%
23.2-32.7	4	1.50%
32.8-42.3	22	8.50%
42.4-51.9	27	10.40%
52-61.5	63	24.20%
61.6-71.1	80	30.80%
71.2-80.7	51	19.60%
80.8-90.4	7	2.70%
Total	260	100.00%

**Table94- 3) Distribution of lesion diagnosed by ultrasound**

<b>Lesion type</b>	<b>Frequency</b>	<b>Percent</b>
Mets	112	43.0%
hemangioma	43	16.5
Abscess	16	6.2
hydated cyst	12	4.6
HCC	49	18.8
Cyst	22	8.5
Lymphoma	3	1.2
Adenoma	2	.8
intrahepatic choleangio ca	1	.4
<b>Total</b>	<b>260</b>	<b>100.0</b>

**Table(4- 4) Relationship between Gender and Lesion type**

<b>Gender</b>	<b>Lesion type</b>					
	<b>Mets</b>	<b>hemiangioma</b>	<b>abscess</b>	<b>hydated cyst</b>	<b>HCC</b>	<b>Cyst</b>
female	50	21	4	6	9	11
male	62	22	12	6	40	11
<b>Total</b>	<b>112</b>	<b>43</b>	<b>16</b>	<b>12</b>	<b>49</b>	<b>22</b>



Gender	Lesion type			Total
	Lymphoma	adenoma	intrahepatic Chole	
Female	0	2	1	104
Male	3	0	0	156
Total	3	2	1	260

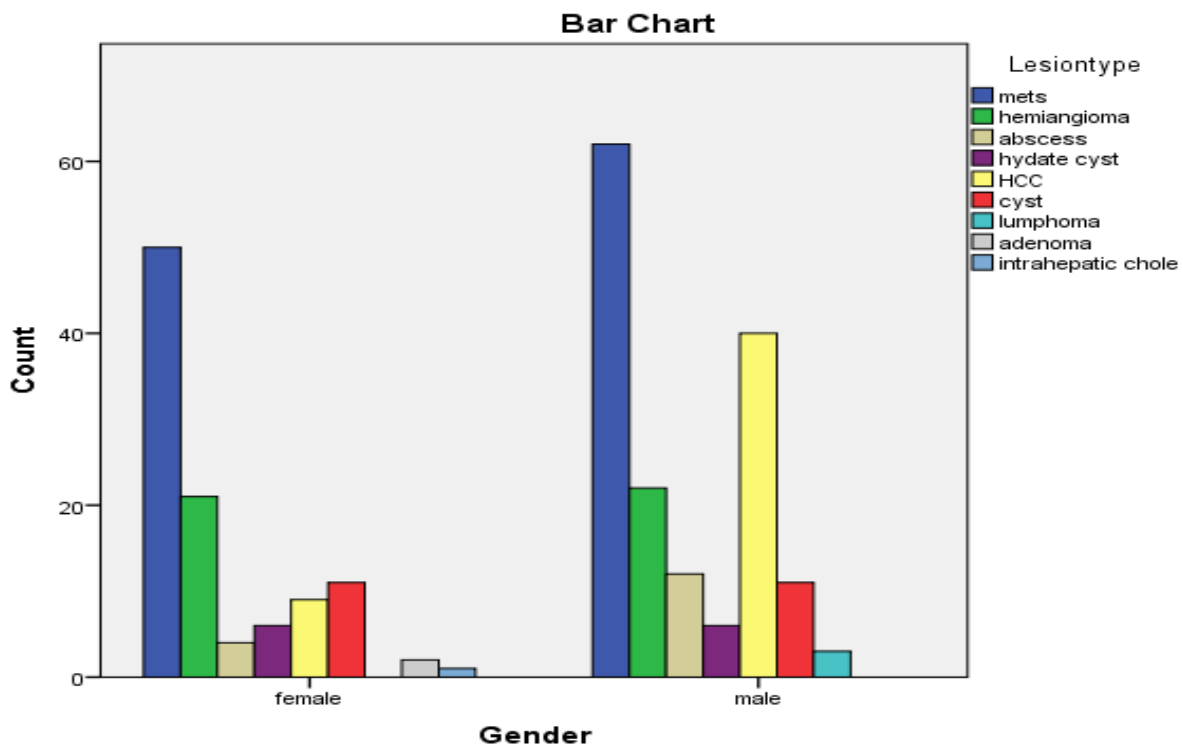


**Figure (4- 1) Relationship between Gender and Lesion type**

**Table(4- 5) Lobar involvement of liver lesions**

<b>Site</b>	<b>Frequenc y</b>	<b>Percent</b>
right lobe	178	68.5
left lobe	23	8.8
both lobe	59	22.7
Total	260	100.0

**Table(4- 6 Distribution of cases based on lesion size**

<b>Size</b>	<b>Frequency</b>	<b>Percent</b>
Small	52	20.0
Middle	22	8.5
Large	116	44.6
different size	70	26.9
Total	260	100.0

**Table94- 7) Relationship between gender and lesion size**

<b>Gender</b>	<b>Size</b>				<b>Total</b>
	<b>Small</b>	<b>Middle</b>	<b>Large</b>	<b>different size</b>	
female	27	8	41	28	104
Male	25	14	75	42	156
Total&14&14	52	22	116	70	260

**Table(4- 8)Relationship between lesion type and lesion size**

Lesion type	Size				
	small	middle	Large	different size	Total
Mets	20	6	29	57	112
Hemangioma	21	8	11	3	43
Abscess	2	4	7	3	16
hydated cyst	0	0	12	0	12
HCC	2	1	44	2	49
Cyst	7	2	9	4	22
Lymphoma	0	1	1	1	3
Adenoma	0	0	2	0	2
intrahepatic chole	0	0	1	0	1
Total	52	22	116	70	260

**Table(4-9) Distribution of cases based on number of lesions**

Lesions	Frequency	Percent
Single	165	63.5
Two	12	4.6
Multiple	83	31.9
Total	260	100

**Table (4- 10) Relatio ship between gender anl lesion size**

Gender	Number of lesion			Total
	single	Two	Multiple	
female	67	4	33	104
male	98	8	50	156
Total	165	12	83	260

**Table(4- 11)Relationship between lesion type and number**

Lesion type	Number of lesions			Total
	single	Two	Multiple	
Mets	41	3	68	112
Hemangioma	37	2	4	43
Abscess	11	3	2	16
hydated cyst	11	1	0	12
HCC	45	1	3	49
Cyst	16	2	4	22
Lymphoma	2	0	1	3
Adenoma	1	0	1	2
intrahepatic chole	1	0	0	1
Total	165	12	83	260

**Table( 4-12)Chi-Square Tests**

	Chi <sup>2</sup> value	p-value (2-sided)
Pearson Chi-Square	88.418	.000
Likelihood Ratio	93.341	.000
Linear-by-Linear Association	37.968	.000
N of Valid Cases	260	

**Table( 4-13) Distribution of cases based on shape of lesions**

Lesion Shape	Frequency	Percent
Rounded	208	80
Oval	14	5.4
Irregular	9	3.5
Rounded halo	7	2.7
Rounded&thickwall	8	3.1
Rounded&sept	2	0.8
Irregular&hallo	3	1.2
Irregular&thickwall	4	1.5
Irregular &septation	5	1.9
Total	260	100

**Table(4- 14) Distribution of cases based on shape of lesions**

Lesion type	SHAPE				
	rounded	Oval	irregular	Rounded+hallo	Rounded+thickwall
Mets	104	7	1	0	0
Hemangioma	37	5	1	0	0
Abscess	5	0	0	0	8
hydated cyst	3	1	0	0	0
HCC	32	0	7	7	0
Cyst	21	1	0	0	0
Lymphoma	3	0	0	0	0
Adenoma	2	0	0	0	0
intrahepatic chole	1	0	0	0	0
Total	208	14	9	7	8

**Table(4-14)Distribution of cases based on shape of lesions**

Lesion type	SHAPE			
	rounded+sept	irregular+hallosi	irregular+thickw	irreular+septati
	pt	gn	all	on
Mets	0	0	0	0
Hemangio ma	0	0	0	0
Abscess	0	0	3	0

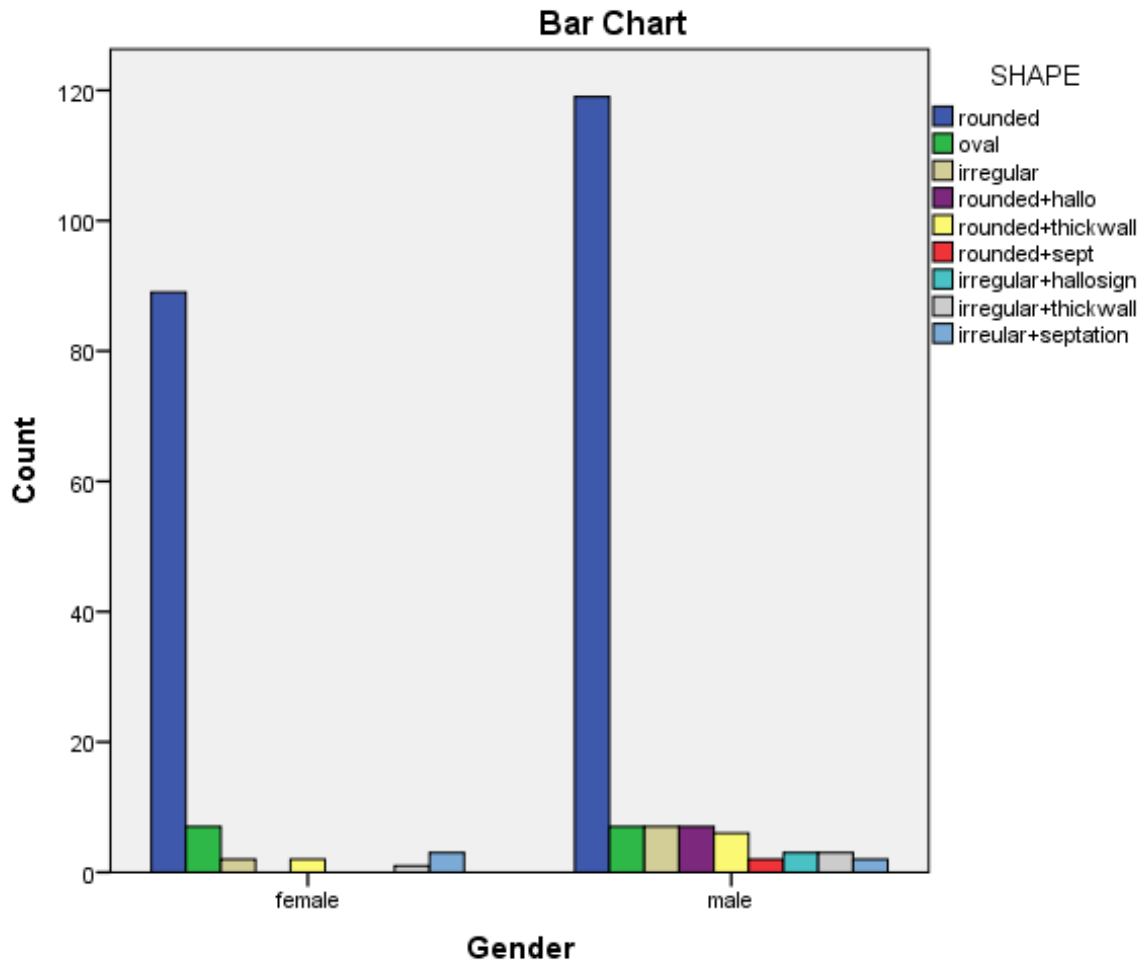
hydated cyst	2	0	1	5
HCC	0	3	0	0
Cyst	0	0	0	0
Lymphoma	0	0	0	0
Adenoma	0	0	0	0
intrahepatic chole	0	0	0	0
Total	2	3	4	5

**Table(4- 15) Distribution of cases based on shape of lesions**

Gender	SHAPE					
	Rounde d	ova l	Irregula r	rounded+hall o	rounded+thickwa ll	rounded+se pt
Female	89	7	2	0	2	0
Male	119	7	7	7	6	2
	208	14	9	7	8	2

**Table(4- 15) Distribution of cases based on shape of lesions**

Gender	SHAPE			Total
	irregular+hallosign	irregular+thickwall	irreular+septation	
Female	0	1	3	104
Male	3	3	2	156
Total	3	4	5	260

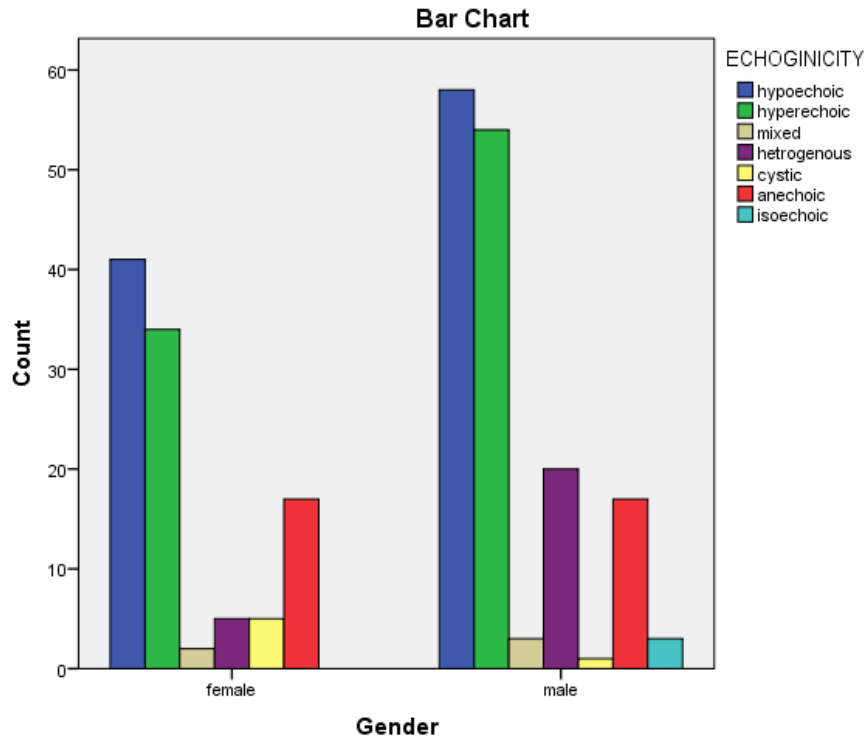


**Figure( 4- 2) Distribution of cases based on shape of lesions**

**Table(4-16) Relationship between the gender and echogenicity**

Gender	ECHOGINICITY							Total
	Hypo echoic	Hyper echoic	Mixed	Heterogeneous	Cystic	Anechoic	Isochoric	
Female	41	34	2	5	5	17	0	104
Male	58	54	3	20	1	17	3	156
Total	99	88	5	25	6	34	3	260





**Figure( 4-3) Distribution of cases based on echgenicity of lesions**

**Table(4-17) Distribution of cases based on echgenicity of lesions**

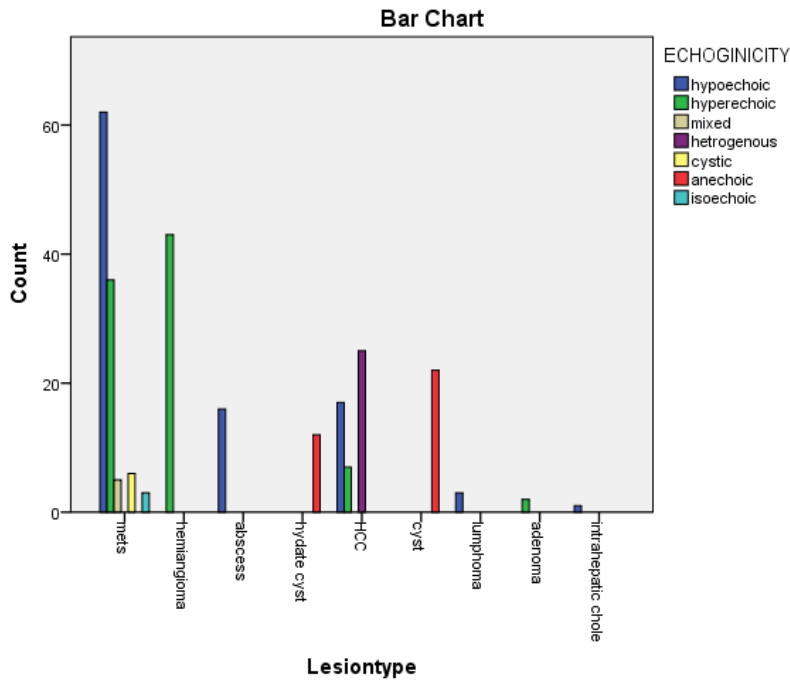
<b>Echogenicity</b>	<b>Frequenc y</b>	<b>Percent</b>
Hypo echoic	99	38.1
hyper echoic	88	33.8
Mixed	5	1.9
heterogeneous	25	9.6
Cystic	6	2.3
Anechoic	34	13.1
Isochoric	3	1.2
<b>Total</b>	<b>260</b>	<b>100.0</b>

**Table (4-18) Relationship between the lesion type and echogenicity**

Lesion type	ECHOGENICITY				
	Hypo echoic	Hyper echoic	Mixed	heterogeneous	Cystic
Mets	62	36	5	0	6
Hemangioma	0	43	0	0	0
Abscess	16	0	0	0	0
hydated cyst	0	0	0	0	0
HCC	17	7	0	25	0
Cyst	0	0	0	0	0
Lymphoma	3	0	0	0	0
Adenoma	0	2	0	0	0
intrahepatic chole	1	0	0	0	0
Total	99	88	5	25	6

**Table(4- 19) Relationship between the lesions type and its echogenicity**

Lesion type	ECHOGENICITY		Total
	Anechoic	Isochoric	
Mets	0	3	112
Hemangioma	0	0	43
Abscess	0	0	16
hydated cyst	12	0	12
HCC	0	0	49
Cyst	22	0	22
Lymphoma	0	0	3
Adenoma	0	0	2
intrahepatic chole	0	0	1
Total	34	3	260



**Figure(4- 4) Relationship between the lesion type and echogenicity**

**Table(4- 20) Distribution of cases based on vascularity of lesions**

vascularity	Frequency	Percent
Peripheral	20	7.7
Central	6	2.3
no flow	16	6.2
not assessed	218	83.8
Total	260	100

**Table(4- 21)Relationship between Lesion type \*and vascularity**

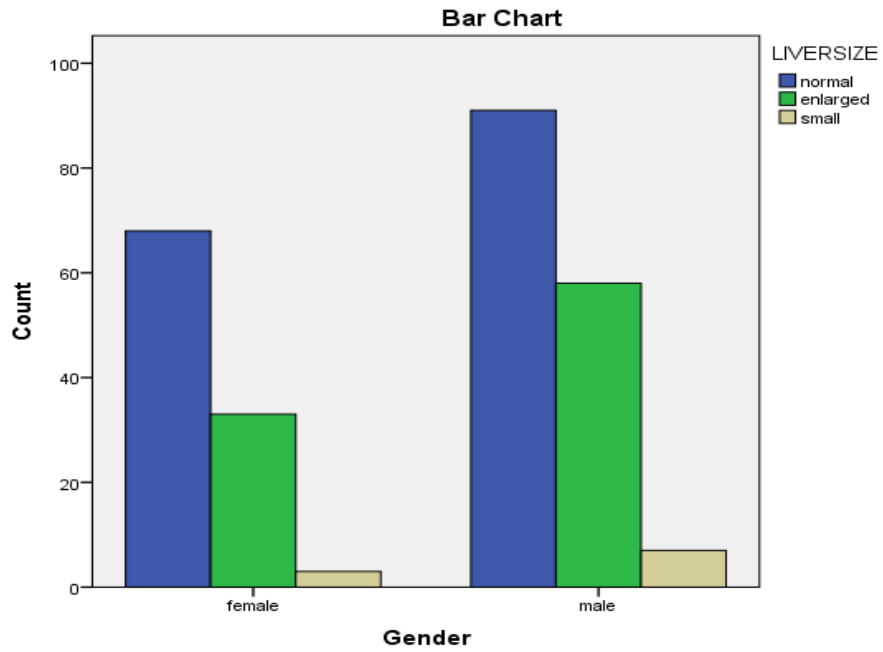
Lesion type	VASCULARITY				Total
	peripheral	central	no flow	not assessed	
Mets	15	0	4	93	112
Hemangioma	1	0	2	40	43
abscess	1	0	1	14	16
hydated cyst	0	0	1	11	12
HCC	3	6	6	34	49
Cyst	0	0	1	21	22
lymphoma	0	0	0	3	3
adenoma	0	0	1	1	2
intrahepatic chole	0	0	0	1	1
Total	20	6	16	218	260

**Table(4- 22) Distribution of lesions based on liver size table**

Liver size	Frequency	Percent
normal	159	61.2
enlarged	91	35
Small	10	3.8
Total	260	100

**Table(4- 23) Relationship between gander and liver size**

Gender	LIVERSIZE			Total
	Normal	Enlarged	Small	
Female	68	33	3	104
Male	91	58	7	156
Total	159	91	10	260



**Figure( 4-5) Relationship between gander and liver size**

**Table( 4-24) Relation between lesion type and liver size**

	LIVERSIZE			Total
	Normal	Enlarged	Small	
Mets	55	57	0	112
Hemangioma	41	1	1	43
Abscess	14	2	0	16
hydated cyst	10	2	0	12
HCC	14	26	9	49
Cyst	21	1	0	22
Lymphoma	1	2	0	3
Adenoma	2	0	0	2
intrahepatic chole	1	0	0	1
Total	159	91	10	260

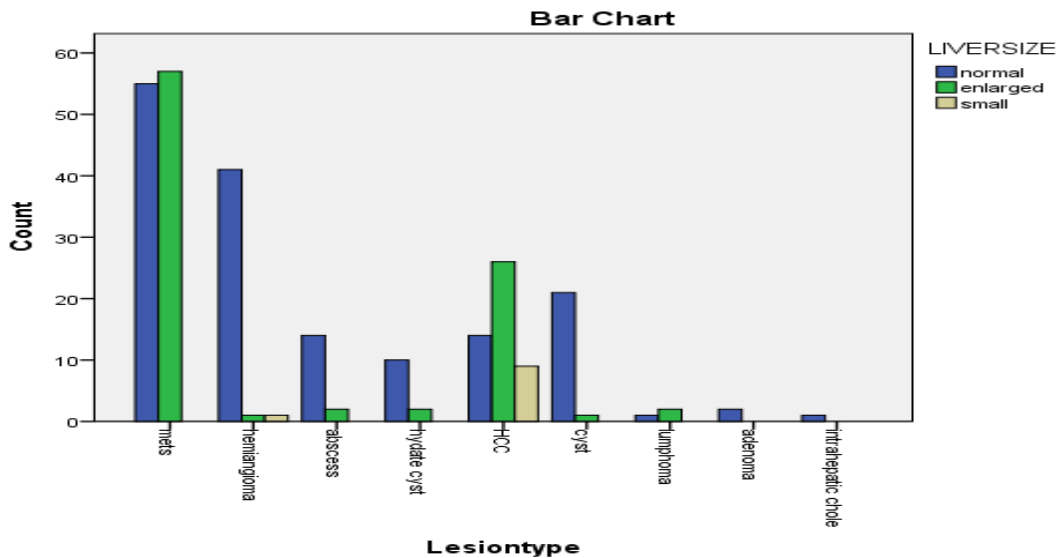


**FigURE (4- 6) Relationship between gander and liver size**

**Table(4- 25) Relationship between gander and liver texture**

Gender	LIVERTEXTURE		Total
	Normal	Coarse	
Female	89	14	104
Male	114	42	156
Total	204	56	260

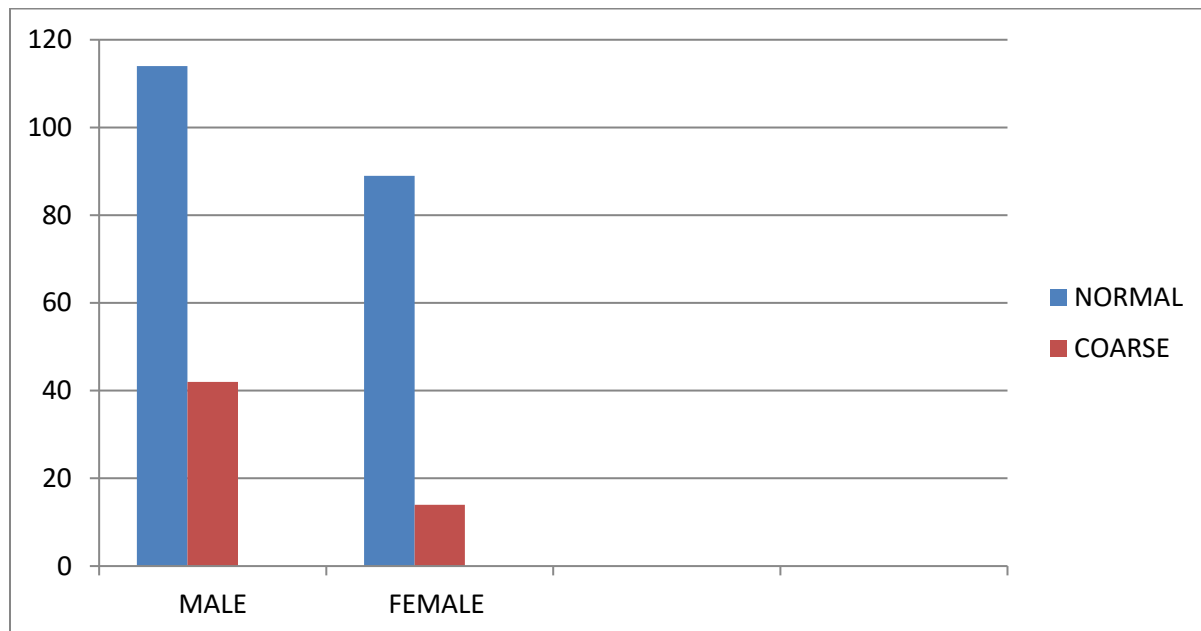


**Figure (4- 7) Relationship between gander and liver texture**

**Table(4- 26) Relationship between lesion type and liver texture**

Lesion type	LIVERTEXTURE		Total
	normal	Coarse	
Mets	83	29	112
Hemangioma	41	2	43
Abscess	16	0	16
hydated cyst	12	0	12
HCC	24	25	49
Cyst	22	0	22
Lymphoma	3	0	3
Adenoma	2	0	2
intrahepatic chole	1	0	1
Total	204	56	260

**Table (4-27) Relationship between gender and right lobe angle**

Gender	RTLOBELANGLE		Total
	Triangle	Rounded	
Female	67	37	104
Male	96	60	156
Total	163	97	260



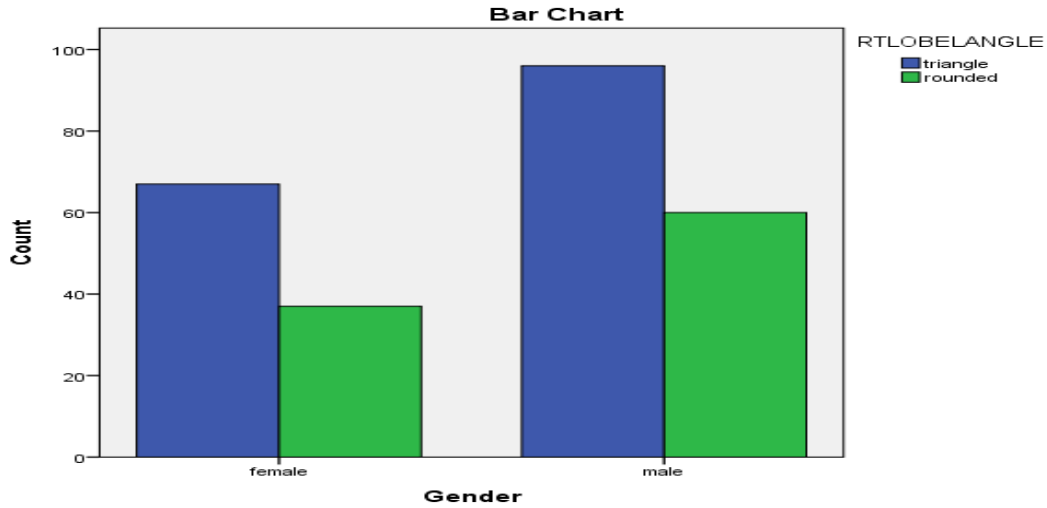
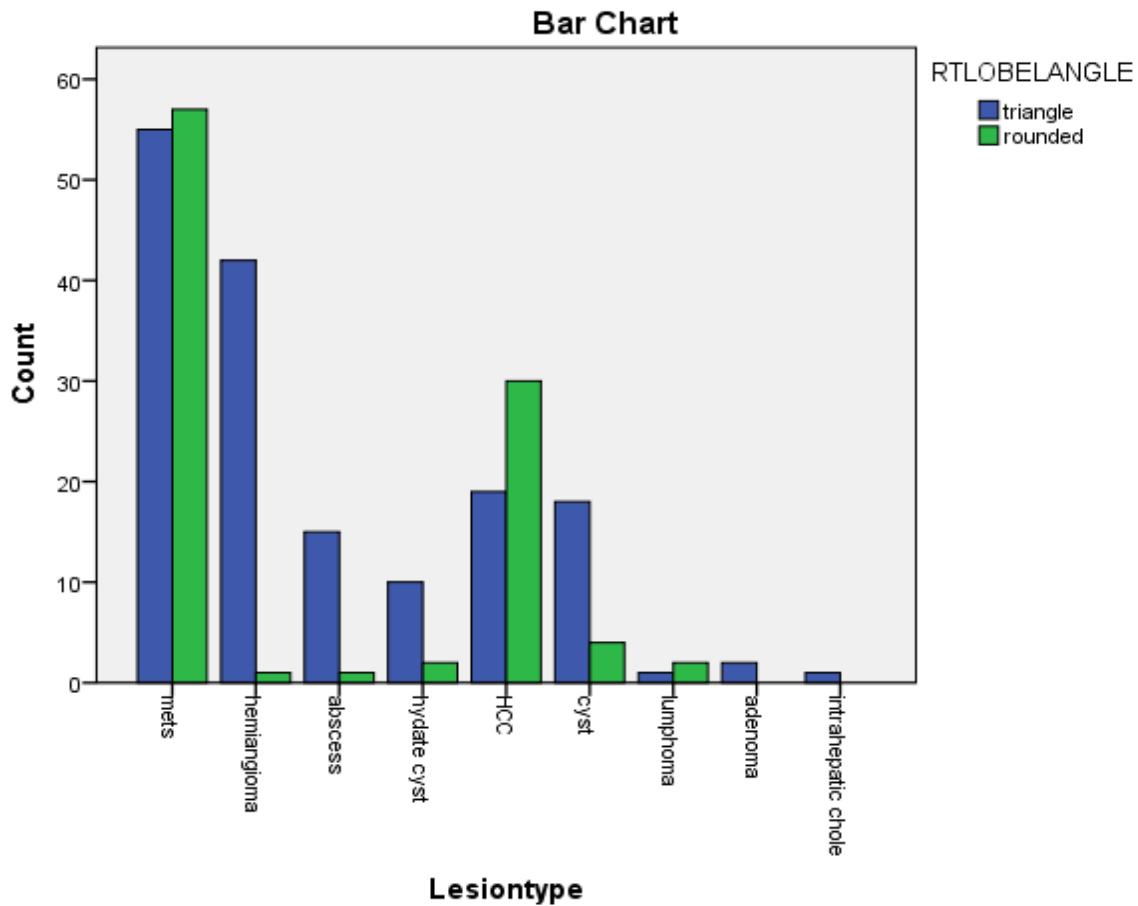


**Figure (4- 8) Relationship between gender and right lobe angle**

**Table (4- 28) Relationship between lesion type and right lobe angle**

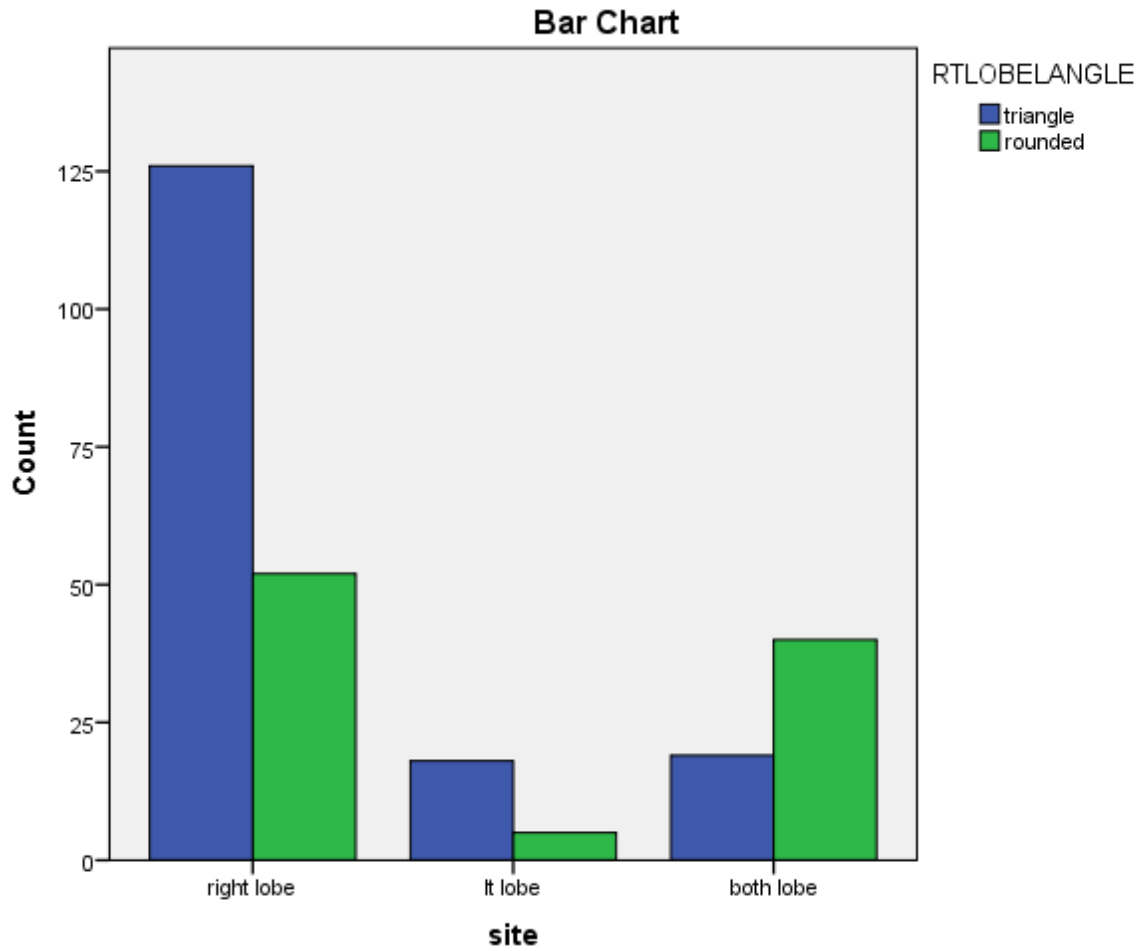
Lesion type	RTLOBELANGLE		Total
	Triangle	rounded	
Mets	55	57	112
Hemangioma	42	1	43
Abscess	15	1	16
hydated cyst	10	2	12
HCC	19	30	49
Cyst	18	4	22
Lymphoma	1	2	3
Adenoma	2	0	2
intrahepatic chole	1	0	1
Total	163	97	260



**Figur (4- 9) Relationship between lesion type and right lobe angle**

**Table( 4-29) Relation between lesion site and right lobe angle**

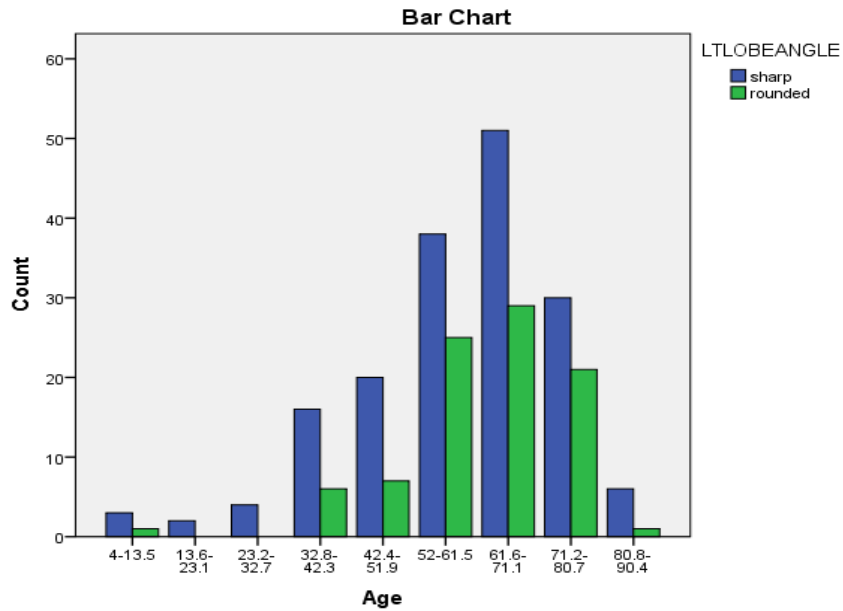
site	RTLOBELANGLE		Total
	Triangle	Rounded	
Right lobe	126	52	178
Lt lobe	18	5	23
Both lobe	19	40	59
Total	163	97	260



**Figure( 4-10) Relation between lesion site and right lobe angle**

**Table (4- 30) Relationship between gender and left lobe angle**

Gender	Lt LOBEANGLE		Total
	Sharp	Rounded	
	Female	69	
Male	101	55	156
Total	170	90	260



**Figure( 4- 11) Relationship between gender and left lobe angle**

**Table (4- 3) 1Relationship between lesion type and left lobe angle**

Lesion type	LTLOBEANGLE		Total
	Sharp	Rounded	
Mets	58	54	112
Hemangioma	41	2	43
Abscess	14	2	16
hydated cyst	11	1	12
HCC	21	28	49
Cyst	20	2	22
Lymphoma	2	1	3
Adenoma	2	0	2
intrahepatic chole	1	0	1
Total	170	90	260

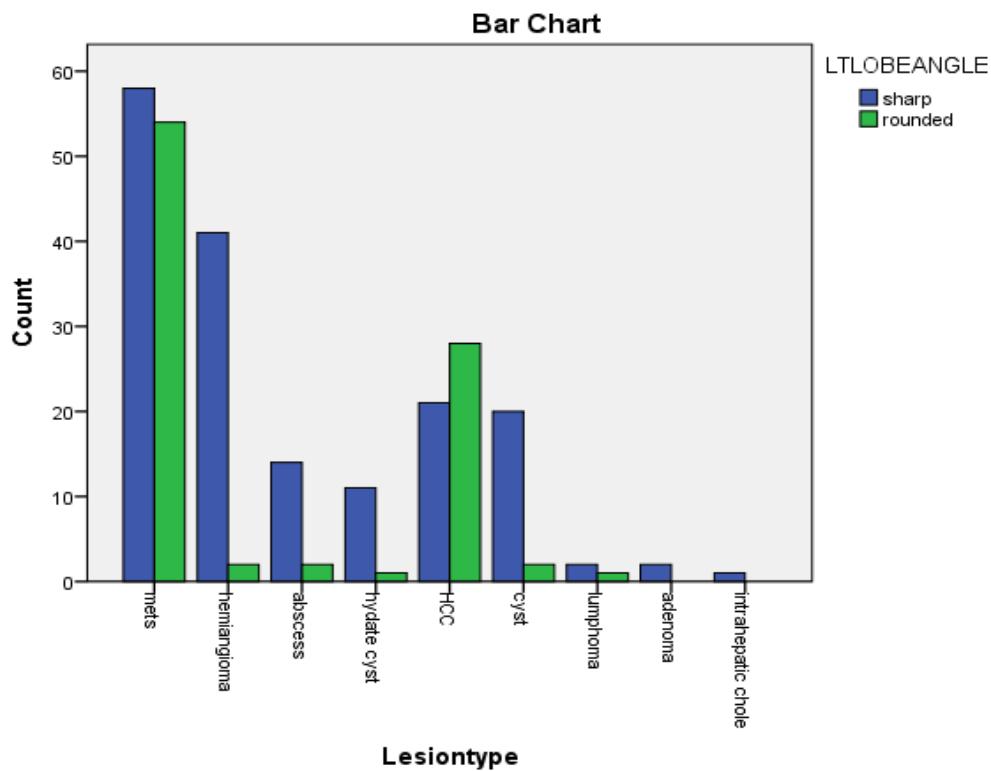


**Figure (4- 12) Relationship between lesion type and left lobe angle**

**Table 4-33 Relationship between lesion site and left lobe angle**

Site	Lt LOBEANGLE		Total
	Sharp	Rounded	
Right lobe	134	44	178
Lt lobe	14	9	23
Both lobe	22	37	59
Total	170	90	260

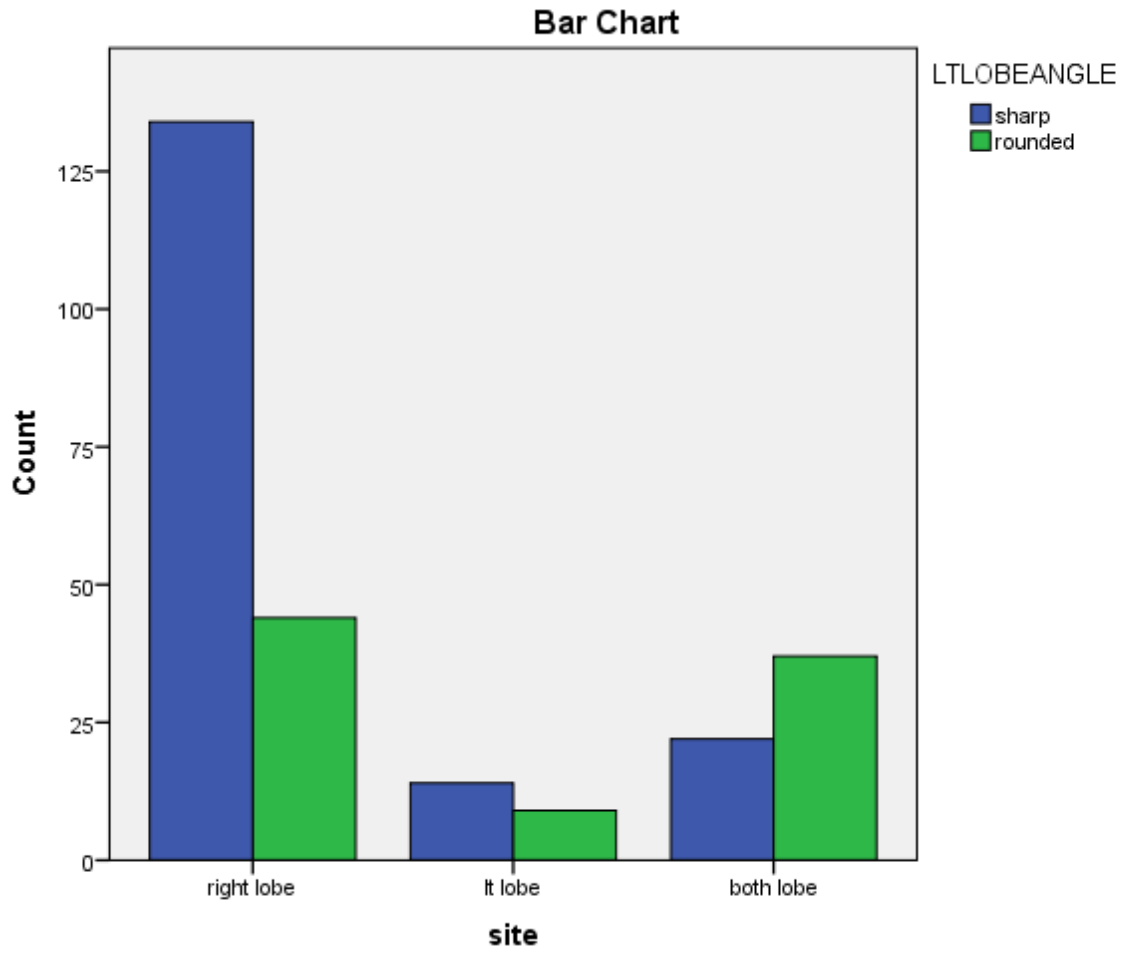
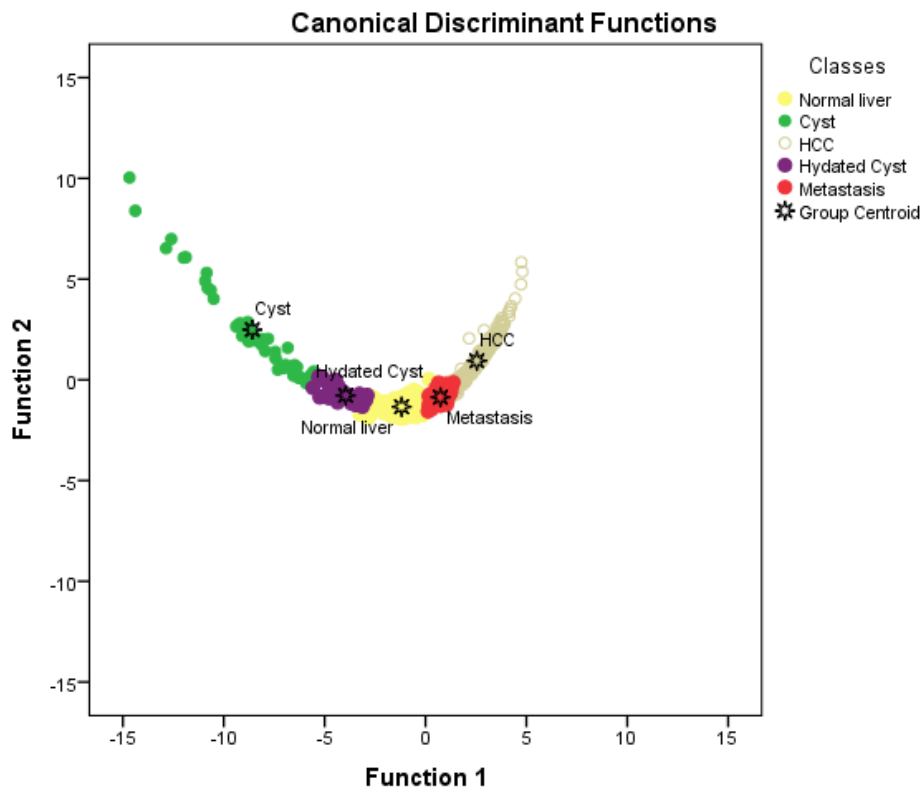


**Figure (4-13) Relationship between lesion site and left lobe angle**



**Figure(4-14) Scatter plot of the classes using discriminant function and center of classes**

**Table 4-34 Classification matrix of the original group and the predicted group using discriminant function**

Classes	Predicted Group Membership					Total
	Normal liver	Cyst	HCC	Hydated Cyst	Metastasis	
Normal liver	<b>99.2%</b>	0.0	0.0	0.0	.8	100.0
Cyst	0.0	<b>75.6%</b>	0.0	24.4%	0.0	100.0
HCC	0.0	0.0	<b>81.4%</b>	0.0	18.6	100.0
Hydated Cyst	0.0	0.0	0.0	<b>100.0%</b>	0.0	100.0
Metastasis	0.0	0.0	0.0	0.0	<b>100.0%</b>	100.0

89.4% of original grouped cases correctly classified

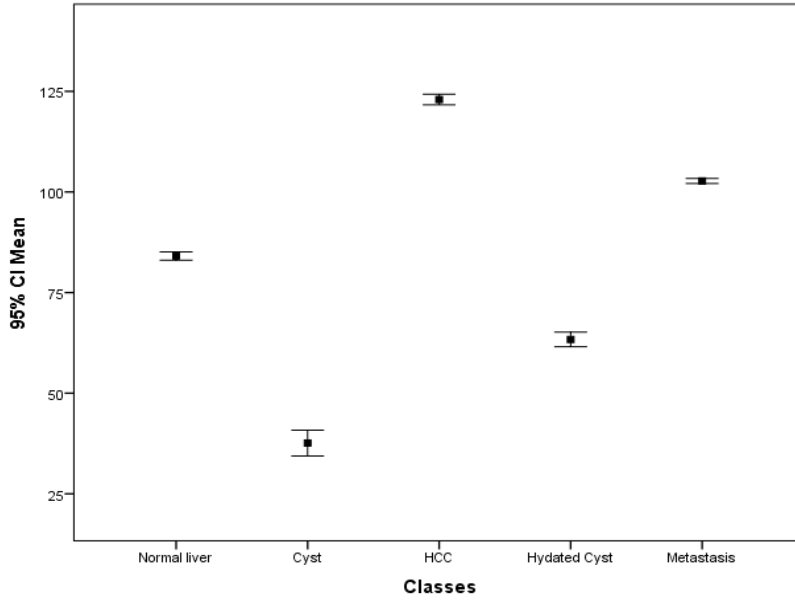
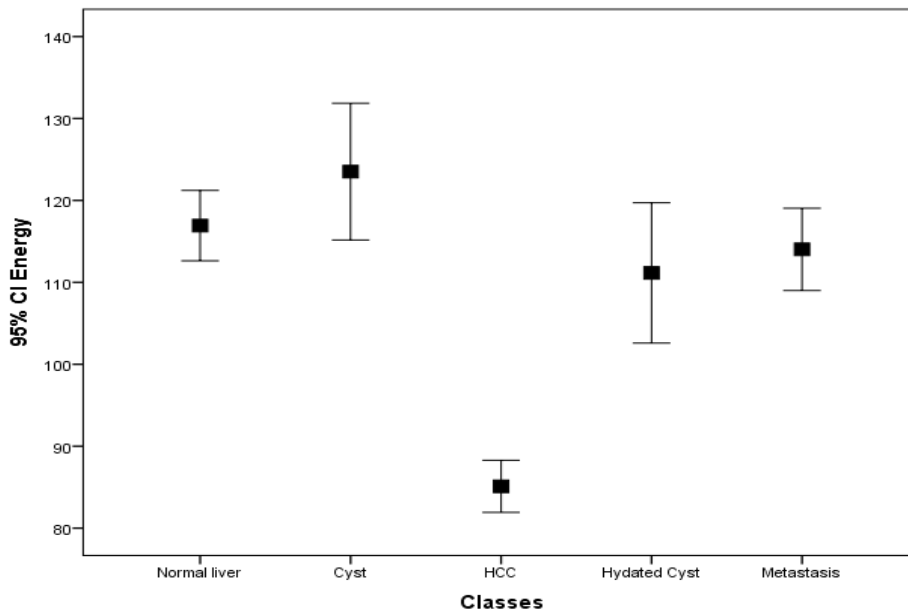
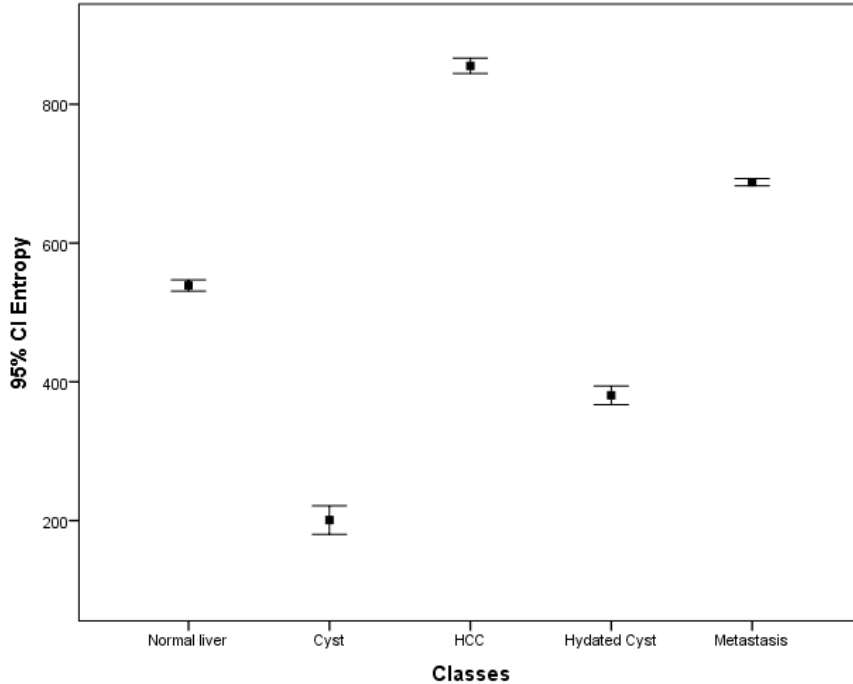


**Figure (4-15) An error bar of 5 classes using the mean feature with the standard error**



**Figure(4-16) An error bar of 5 classes using the energy feature with the standard error**





**Figure(4-17) An error bar of 5 classes using the entropy feature with the standard error**

in conclusion the result of this study dictate that to identify the tissue in the liver as normal, Cyst, HCC, Hydated cyst or METS the following equation should be used where the vote will be to the highest value

$$\text{Normal liver} = (35.6 \times \text{mean}) + (0.2 \times \text{Energy}) + (-4.2 \times \text{Entropy}) - 365.8$$

$$\text{Cyst} = (25.7 \times \text{mean}) + (0.19 \times \text{Energy}) + (-3.1 \times \text{Entropy}) - 185.4$$

$$\text{HCC} = (35.8 \times \text{mean}) + (0.17 \times \text{Energy}) + (-4.2 \times \text{Entropy}) - 411.0$$

$$\text{Hydated cyst} = (32.95 \times \text{mean}) + (0.185 \times \text{Energy}) + (-3.95 \times \text{Entropy}) - 303.19$$

$$\text{METS} = (36.4 \times \text{mean}) + (.205 \times \text{Energy}) + (-4.31 \times \text{Entropy}) - 400.4$$

**z**

## Chapter five

### Discussion, Conclusion and Recommendations

#### 5-1 Discussion

This study aimed to characterized the liver lesions using ultrasound and texture analysis and gray level intensities so far for classification of lesions and liver in ultrasound images, comprises of 260 patients with different types of primary and malignant liver lesions underwent successful abdominal ultrasound for a period of three years conducted in the department of radiology at Ibn Sina teaching hospital and Dr Osman Alwahab private clinic. These patients were subjected for ultrasound evaluation and some of them confirmed by CT and FNA , The various types of liver lesions encountered in this study were liver metastases, hepatocellularcarcinoma,lymphoma,intrahepaticcholangiocarcinoma,abscesses,haemangioma,simplecysts,hydratedcystsand adenoma The followed observations were made :156 (60%) out of 260 patients were male and104 (40%) patients out of 260 were female. males had increased predilection with a male to female ratio of 1.5 -1. These finding supported by Thimmaiah 2013, and Hapani et al 2014. ( **Table 4-1**)

The study showed that the age grouped range between 61,6 - 71,1 years old had the maximum incidence with 80(30.8%) cases, most of them were in 39 cases as Mets . and between (13.6 -23.1) showed the lower incidence with 2 (.8%) cases, while Thaimiah 2013, and Hapani et al2014 reported the maximum incidence of age grouped were between (41 – 50). with 39 (39%), 18(36%) and below 10 showed lowest incidence with 5(4.8%), 1(2%) cases. The differences due to higher population used in this study. (**Table 4-2**)

Out of the total 260 cases the most common liver lesions discovered by ultrasound were 112 (43%) cases as metastases, appear more in male 50 cases than female 26

cases. followed by 49(18.85%) cases as HCC more in male 40 cases than male 9 cases, 43(16.5%) cases as haemangioma more in male 22 cases than female 21 cases, 22(8.5% ) as cyst,16(6.2%) cases as abscesses more in male 12 cases than female 4 cases, 12(4.6) cases as hydrated cyst while the other as lymphoma all of three in male, adenoma all of two female, and intrahepatic cholangi carcinoma in one patients, with 3 (1.2%), 2 (.8%). and1 (.4%) respectively. so liver metastases have higher incidence followed by HCC. According to Hapani etal 2014 whom reported that out of 50 cases t he most lesions were 18(36%) liver abscesses , 8(16%) haemangioma, , 7(14%) metastases, 6(12%) cyst ,4(8%) primary liver tumors, and3(6%) hydrated cyst in population of 50 patients. **Table (4-3),(4-4) and (fig 4-1)**

According to lobar involvement of liver lesions, there was 178 cases (68.5%) had right lobe involvement 23 cases (8.8%) had left lobe involvement, and 59 cases (22.7%) involved both lobes. the highly affected of right lobe involvement due to streaming of portal venous blood from more frequently and more heavily infected right side of colon specially in liver abscesses, and much greater volume of right lobe. This finding semi like study done by Thaimiah et al 2013 whom they found that 64%had right lobe involvement,11% had Lt lobe involvement and 23% involved both lobes. **Table(4- 5)**

Regardless to the size of liver lesions, out of 260 cases there were 116 lesions (44.6%) (75 male, 41 female) had largest size, most of them appear in 44 HCC. 70 lesions (26.9%). 42 male ,28 female had different sizes , mostly in 57 Mets . 52 lesions (8.5%)(25 male, 27 female) had small size , mostly in 21 haemangiomas

and middle size in 22 (20.0%)(14 male ,8 female of lesions specially in 8 haemangiomas. **Table (4-6),(4-7)and(4-8)**

Out of 260 lesions 165 (63.5%) (98 male 67 female) were single followed by 83(31.9%)were multiple while the remaining 12(4.6%) were tow in number. **Table (4-9)and(4-10)**

The study shows that among 260 lesions the majority was 45 lesions of 165 (63.5%) discovered as HCC were single in number followed by 68 lesions of 83(31.9%) as Mets were multiple while the remaining lesions three of 12 (4.6%) were Mets 3 and the other were benign lesions were tow in number. a significant correlation( $p= 0.000$ ) noted between lesion type and number. **Table (4-11)and(4-12)**

The majority of cases of liver lesions had round shape in 208 cases (80%) most of them founded in male as liver metastases(104) ,the others described 14 (5.4%)as oval mostly in metastases(7) , 9(3.5%) as irregular mostly in HCC(7), 8(3.1%) as round+ thick wall all in abscesses , 7 (2.7%) as round+hallosign all in HCC, while the remaining 14 cases described as 5 cases(1.9%)was irregular+septation all in hydrated cyst , 4 cases(1.5%) was irregular+thickwall mostly in abscesses , 3 cases(12%) was irregular+hallosign, all in HCC and 2 cases (.8%)was round+septation all in hydrated cyst .**Tables ( 4-13),(4-14),(4-15) and (fig4- 2)**

In relationship between the lesions type and its echogenicity out of 260 lesions discovered there were 156 (60%)were male and 104(40%)were female. 99 cases ,the echogenicity appear hypoechopic more in female 58 cases than male in 41 cases . the majority 62 cases were hypoechopic in metastases (METS) due to

vascularity ,replication of cells and fat or fluid containing of original cancer. out of 88 lesions appear hyper echoic in 54 male , and 34 female most of them were 43 hyper choc appear in haemangioma, which thought to be due to multiple interface between walls of cavernous sinuses and blood contained within. The total of 25 lesions appear heterogeneous echo pattern in 25 male and 5 female, all of them appear heterogynous in hepatocellular carcinoma (HCC) as a result of necrosis and fibrosis. Out of 34 17 male ,17 female, appear an echoic more in 22 cyst and 12 hydated cyst and few were appear as mixed 6 cases in Mets as cystic and 3 isochoric also in met .**(Tables (4-16),(4-17),(4-18),(4-19),Fig(4-3)and Fig(4- 4)**

In relationship between the diagnosis and the color flow Doppler pattern , out of 260 lesions showed 20 lesions(7.7%) with peripheral 15 of them were Mets ,16 lesions ( 6.2%) with no flow most of them 6 in HCC ,4 in Mets while the remaining in benign lesions. , 6 lesions (2.3%) with central flow all in HCC, while the remaining 218 lesions (83.8%) were not assessed due to non availability of Doppler scan . **table(4-20)and(4-21)**

In relationship between liver size and lesion type out of 260 lesions the study showed that 159(61.2%) lesions with normal liver size in 91 male and 68 female, these included 55 (49%) of 112 Mets 14(28.5%) of 49 HCC ,one (100%)of one cholangiocarcinoma one(100%)of one lymphoma and 88( 93% )of 95 benign lesions. 91(3.5%) lesions with enlarged liver size in 58 male and 33 female ,these included 57(50.8% )of 112 Mets ,26(53%) Of 49 HCC ,one(100%) of one cholangiocarcinoma two(66.7%) of three lymphoma and 6(6.3%) of 95 benign lesions . and 10(3.8%) lesion with small liver size in 7 male and 3 female which included 9(64%) of 14 HCC and one(2.4%) of 41 haemangioma. Most of enlargement of liver size according to multiple liver metastases due to strengthened

of the liver . the small size according to HCC due to shrunken cirrhotic liver. Metastases was most common detectable affected liver size followed by HCC. There is a significant correlation at ( $p=0.000$ ) between lesion type and liver size (**Tables (4-22),(4-23),(4-24),Fig(4-5)and(4-6)**)

Regardless to lesion type and liver texture among 260 patients ,there were 204 male and 56 female .111 of 204 patients (78.4%) with malignant liver lesions had normal liver texture while the remaining 93 patients with benign liver lesions .56 patients (21.5%) 42 were male while 14 were female which includes 54 patients with malignant liver lesions had coarse liver texture and two had coarse liver texture in patients with haemangioma. **Tables ( 4-25),(4-26)and Fig(4-7)**

According to right liver lobe angle among 260 patient 104 (60%) were female and 156 (40%) were male. 163 patients had triangled right lobe angle, in 76 patient with malignant liver lesions in most cases of Mets in 55 of 76 cases, and in 78 patients with benign liver lesions in most cases of haemangioma in 42 of 78 cases, also it triangled in 126 patients where the lesion involved right liver lobe , in 18 patients where the lesion involved left liver lobe and in 19 patients where the lesion involved both liver lesions. 97 patients had rounded right liver lobe angle, in 89 patients with malignant liver lesions and in 8 patient with benign liver lesions , also it rounded in 52 patients where the lesion involved right liver lobe, in 23 patients where the lesion involved left liver lobe and in 40 patients where the lesion involved both liver lobe (**Tables (4- 27),(4-28),(4-29),Fig (4- 8)(4-9)and(4-10)**)

According to left liver lobe angle among 260 patients104 (60%) were female and 156 p (40%) were male. 170 patients had sharp lt lobe angle more in male 101

than female 69. The lt lobe angle appear sharp in 88 patient with malignant liver lesions in most cases of liver Mets in 58 of 88 lesions and in 82 patients with benign liver lesions more in haemangioma, also it appear sharp in 134 patients where the lesion involved right liver lobe , in 114 patients where the lesion involved left liver lobe and in 22 patients where the lesion involved both liver lesion. The remaining 90 patients had rounded left liver lobe angle more in male 55 than female 35. 83 patients with malignant liver lesions and in 7 patient with benign liver lesions , also it rounded in 44 patients where the lesion involved right liver lobe, in 9 patients where the lesion involved left liver lobe and in 37 patients where the lesion involved both liver lobe. **(Tables (4- 30),(4-31),(4-33),Fig(4-11),(4-12) and(4-13)**

Liver lesions are common on pathologic or imaging evaluation of liver and include the variety of benign and malignant lesions. This study revealed individually that the most common liver lesions were metastases more in male, this can be attributed to its large size, high rate of blood flow and double perfusion by portal vein and hepatic artery, It characterized hypo echoic, multiple, with different sizes, it more involved right liver lobe. the liver had normal echo texture and enlarged size with more sharp left lobe angle and most rounded right lobe angle in more patients with liver metastases which had peripherally vascularized.

The second most commonly liver lesions were hepatocellular carcinoma more founded in male in older patients. Son graphically most of them characterized as heterogeneous echo pattern as a result of necrosis and fibrosis. They appeared rounded in shape, and irregular outlines with halo sign, more had large size single and central vascularity. The liver tends to be coarse echo texture, enlarged size with rounded right liver lobe angle in more cases. the third common liver lesion

types were haemangioma more in male . most of them characterized as hyper echoic , single, rounded, small size, no flow. It more affected right liver lobe with triangle angle, and sharp left liver lobe angle the liver had normal size and echogenicity in more cases. The fourth lesion types were liver cysts which characterized as anechoic single, round, large size with normal liver size and echotaxture in more cases .it more affected right liner lobe with triangle lobe angle and sharp Lt lobe angle more in male than female. Regardless to liver abscesses there was strong tendency for male they characterized as more hypoechopic, single ,rounded in shape ,large size with normal liver size and echo texture .It more affected right liver lobe with triangle right lobe angle .

Hydated cysts were frequently involved the liver in the present study ,they were more founded in male , characterizes as purely cystic, single, large size, rounded with septation, the liver had normal size and echotexture with right lobe involvement with triangle angle in more cases ,the remaining liver lesions discovered in the study were rare as lymphoma, adenoma ,and intrahepatic choliangiocarcinoma. .

**Related to texture analysis and gray level intensities:** The classification concerned the textural features extracted from all images that represent five classes (normal liver, cyst, hydrated cyst, hepatocelullar carcinoma and liver metastases) of the study using first order textural features , using a 3X3 window which created in order to scan the image of ultrasound containing the classes, these textural features include: mean, entropy and energy, which were calculated for all images and then the data were ready for discrimination which was performed using step-wise technique in order to select the most significant feature that can be used to classify the lesions in ultrasound liver images which give best discrimination



during the scan for five selected classes and the result showed that there is a well concentration of features around the classes centers which give a remarkable difference among the classes. Fig (4-14) and table(4-31) shows the classification matrix of the original group and predicted group using discriminant function presented the classification accuracy of each classes in which 92.2% of normal liver was correctly classified and 75.6%,81.4%,100.0%, and 100.0% classification sensitivity for liver cyst, HCC, hydrated cyst, and liver metastases respectively. With highest predictive overall accuracy of 89.1% .

The results are represented that there is a well concentration of features around the class centers which give a remarkable difference among the five classes. From the discriminant power point of view in respect of applied features the entropy can be differentiate between all classes successfully similarly the mean. (**Fig (4-15)and(4-17)**)

Mean and entropy can successfully differentiate between cyst and HCC,from the rest of tissue but they give spar differentiation between metastases and HCC because they both had similar average group level .heterogeneity and overlapping of textural features. Finally the energy gives more emphases on HCC than the other tissue type as in fig 4-16

In conclusion the result of this study dictate that to identify the tissue in the liver as normal, Cyst, HCC, Hydated cyst or METS the multiple discriminant linear regression analysis equations can be used to classify the liver in the mentioned classes where the vote will be for the higher value

## **5-2 Conclusion:**

The study concluded that the most common liver lesions were metastases followed by hepatocellular carcinoma, haemangioma, liver cysts, Hydated cysts were frequently involved the liver in the present study while the remaining liver lesions discovered in the study were rare as lymphoma, adenoma, and intrahepatic cholangiocarcinoma.

The study showed that the age grouped range between 61.6 – 71.1 years had the maximum incidence, and between 13.6 -23.1 showed the lower incidence. It is evident that Ultrasonography has a wide applicability in the diagnosis of liver lesions being a safe, simple, repeatable, and without radiation exposure to the patients. It allows to scan the liver in multiple planes enabling to know the location of lesions and study their echo pattern, it is worthy of being included in a routine diagnostic work.

The texture reveals different underlying patterns of normal liver compared to benign and malignant liver lesions with highest predictive overall classification accuracy of 89.4%. This study dedicates that texture analysis is superior to visual perception systems where texture reveals the change and the difference of the image pattern objectively in respect to the ground truth.

Gray level intensity value can be used a valuable quantitative tool that would be helpful in improving the confidence in liver lesions as well as facilitating more accurate diagnosis, texture analysis can be adopted as a method of classification to describe microscopic changes in the liver which does not reveal itself ultrasonographically.

Normal liver and benign and malignant liver lesions in ultrasound images for simplicity can be diagnosed as normal or abnormal (according to its type) by using the following equation after extracting the associated features using a window of 3X3 pixel from region of interest; the biggest classification score assume the tissue type.

Finally the following equation can be used to classify the liver tissues into one of the following classes where the vote will be to the highest value

$$\text{Normal liver} = (35.6 \times \text{mean}) + (0.2 \times \text{Energy}) + (-4.2 \times \text{Entropy}) - 365.8$$

$$\text{Cyst} = (25.7 \times \text{mean}) + (0.19 \times \text{Energy}) + (-3.1 \times \text{Entropy}) - 185.4$$

$$\text{HCC} = (35.8 \times \text{mean}) + (0.17 \times \text{Energy}) + (-4.2 \times \text{Entropy}) - 411.0$$

$$\text{Hydated cyst} = (32.95 \times \text{mean}) + (0.185 \times \text{Energy}) + (-3.95 \times \text{Entropy}) - 303.19$$

$$\text{METS} = (36.4 \times \text{mean}) + (.205 \times \text{Energy}) + (-4.31 \times \text{Entropy}) - 400.4$$

Excellent discrimination between benign and malignant liver lesions can be established based on the texture characteristics and this serves as a second method to perform more characterization of the lesion.

### **5-3 Recommendations:**

- Liver is a common site affected by the diseases so close follow up by ultrasound screening routinely to exclude the presence of liver disorder or not.
- Patient should be awarded and supported to increase awareness on liver pathology.
- Existing techniques can be applied to classify and differentiate other types of liver lesions.
- More texture features and techniques can be used to improve the performance.
- Texture analysis can be carried out in all ultrasound images where the lesion was visible therefore it can be used for planning process of radiotherapy treatment.
- Initiation of image processing unit in the radiology department can help a lot in activation of image processing project.
- If there is indication of liver disorder by ultrasound screening , the patients image must be analysed by IDL program ,then the histopathology will be done for the confirmation only, if it is not available, no need of it for giving the patients the treatment , because the prediction of U/S and texture analysis tools together is very high;

**Reference:**

Ali. A. Sakr, Magdi Ilias Faris, Mai Ramadan 2014. Automated Focal Liver Lesion Staging Classification Based On Haralick Texture Features and Multi-SVM , pp. 269-285.

Bankman,I. N, 2008: Handbook of Medical Image Processing and Analysis, Academic Press, Second Edition.

Buel JF, Tranchart H, canon R etal, 2010. Management of Benign Hepatic Tumors. Sur, CLIN North AM .; 90-719-735.

Castellano, G, Bonilha, I. Li, LM Cendes, 2004. Texture analysis of medical. F: Clin, Radial .59 (12), pp.1061-1069.

Charlotte van Kesse, 1 C.S.van Kessel, 2012. Optimization of imaging and treatment of patients with focal liver lesions.

Dr. Andrew Dixon et al, 2016. Web site [https:// radio.pedia.org/ articles/ multiple biliary hamartoma -1](https://radio.pedia.org/articles/multiple_biliary_hamartoma-1). Visited on 16.1.2017 10:30 pm.

Deepi Mittal, Vinod Komar, 2011. Neural Network based focal liver lesion diagnosis using ultrasound images. Computerized Medical Imaging and Graphics. Vol 35, pp 315-323.

Deepti Mittal, Anju rani and Ritambhara, 2016. Detection and Classification of Focal Liver Lesions using Support vector machine classifier. Journal of

Biomedical Engineering and Medical Imaging. Volume 3, no 1 February, pp21-34.

Delia Mitrea , Sergio NEDEVSKI, Mihai. SOCACIU, Radu, ADEA. APRIL 2012. The Role of Superior Order GLCM in the Characterization and Recognition of the Liver Tumors from Ultrasound Images. Radio engineering, VOL 21, NO1.

Dorota Duda, 2014. Advances in Computer Science Research, Faculty of Computer Science, Bialystok University of Technology, Białystok, Poland. vol 11, pp, 61-84.

Dr Amir Razaee and Dr Yuranga Weerakkody, et al 2016. Web site: [https://radiopedia.org/articles/simple hepatic cyst](https://radiopedia.org/articles/simple-hepatic-cyst). Visited on 16/1/2017, at 9:30 pm

Dr Bruno, Di Muzio and Yuranga Weekkody et al, 2016. Web site: [https://radiopedia.org/articles/ hepatic haemangioma-3](https://radiopedia.org/articles/hepatic-haemangioma-3). Visited on 20 1 2017 1:00 pm .

Dr Craig Haking and Dr Kosky Jaccop et al, 2016. Web site:

[https://radiopedia.org/articles/ hepatic adenoma](https://radiopedia.org/articles/hepatic%20adenoma). Visited on 20/1/ 2017, at 1:30 pm .

Dr Henry Knipe ,and Dr Alexandra Stanislavsky, et al 2016 .Website:

[https://radiopedia.org/articles/caroli disease](https://radiopedia.org/articles/caroli%20disease) visited on 17/1./2017, at 9:30 am.

Dr henry knipeand dr Jeremy jones etal, 2014. Web site:

[https://radiopedia.org/articles/liver lesions](https://radiopedia.org/articles/liver%20lesions). Visited on 15/1./2017,at 9 am.

Frank Gaillard et al, 2016. Web site:

[https://radiopedia.org/articles/ focal nodular hyperplasia](https://radiopedia.org/articles/focal%20nodular%20hyperplasia), Visited on 20/1/2017, at 5:20 pm.

Frank Gaillard et al, 2016. Web site :

[https://radiopedia.org/articles/ hyper vascular liver lesions](https://radiopedia.org/articles/hyper%20vascular%20liver%20lesions). Visited on 19/ 1/ 2017, at 1:300 pm.

Frank Gaillard etal, 2016. Website:

[https://radiopedia.org/articles/hepatic metastases-1](https://radiopedia.org/articles/hepatic%20metastases-1). Visited on 19/1/2017,at2:00 pm.

Frank Gaillard et al, 2016. Web site:

[https://radiopedia.org/articles/ choliangiocarcinoma](https://radiopedia.org/articles/cholangiocarcinoma). Visited on 19/1/2017, at 8:00 pm.

Frank Gaillard et al, 2016.Web site:

[https://radiopedia.org/articles/hepatocellular carcinoma](https://radiopedia.org/articles/hepatocellular%20carcinoma). Visited on19/1/2017,at 2:30 pm.

Frank Gaillard et al, 2017.web site:

[https://radiopedia.org/articles/ hepatic hydrated infections/revision](https://radiopedia.org/articles/hepatic-hydrated-infections/revision) visited on 17/1/ 2017 at 4:30 pm.

Frank Gallard,etal 2016 Web site:

[https://radiopedia.org/articles/ hepatic abscess-1](https://radiopedia.org/articles/hepatic-abscess-1). Visited on 17/1/2017, at 10 am.

Galloway, M.M. 1975. Texture analysis using gray level run lengths. *Comput. Vision Graph.* 4(2), pp. 172-179

Gonzalez, R.C., Woods, R.E. 2002. *Digital Image Processing Second edition*, Reading, MA: Addison-Wesley.

H,N,ggada,AAhidjo,NAjayi,SMmustapha,UPpindiga,ATahir,WGghashau,MKhal  
2006. Correlation between ultrasound finding and ultrasound guided –fine needle aspiration cytology in the diagnosis of hepatic lesions .ANigerian TertiaryHospital

Haralick, R. M., Shanmugam K., Dinstein I, 1973. Textural features for image c

Harlic,R M, 1979. Statistical and structural approaches to texture, *Proc. Of the IEEE* 67(5) , PP ,786-804).

Hiral HapanimDr Jegroti, Dr Anjana Trividi, and Dr Anirudh Chawla. Des.2114  
.Ultrasound evaluation of focal hepatic lesions. *Journal of Dental and Medical Science* .Volume 13, Issue 12 ver. (). PP 40-45).



Hornig, M.H., Sun, Y.N., Lin, X. 2002. Texture feature coding method for classification of liver sonography. *Comput. Med. Imag. Grap* 26(1), pp. 33-42.

Hyung kim, jeong min lee, kwang, April 2009. Computer Aided Image Analysis of Focal Hepatic Lesions in Ultrasonography Preliminary Result Abdominal Imaging, Volume 34, Issue 2: PP.183-191.

Ian Bickle and Aprof Frank Gaillard et al, 2016 .web site:

<https://radiopedia.org/articles/hepatoblastoma>. Visited on 19/ 1/ 2017, at 8 :50 pm

*International Journal of Computer Applications*. (0975-8887), Volume 91- No 8  
April PP

Ishak, k. G, Goodman, Z.D, Slocker JT. 2001, Tumors of Liver and Intrahepatic Ducts.

Jemal A, Siegel R, XUJ et al, 2010. Cancer Statistic. *Ca Cancer j CLIN*, 60:277-300

Jetendra Vermani, vinod kumar naveen kalra & niranjan khandelwal, February 2013. Characterization of Primary and Secondary Malignant Liver Lesions from B-Mode ultrasound. *Journal of Digital Imaging*. The Journal of the Society For Computer Application in Radiology.

Jetendra Vermani, Vinod Kumar Naveen Calva Naranjan Khandelwal, (2014). Neural Net Work Ensemble based CAD system for focal liver lesions from B-mode ultrasound.. *J Digital Imaging* , 27. Pp. 520-537.

Jetendra Virmani ,Vinod Komar ,N.K &Khandelwall,2013. N. PCA-SVM based CAD system for focal liver lesions using B- mode ultrasound images. Defence Science Journal, Vol, 63.pp.470-486

Kerlin P, Davis GL MC, Gill DB et al, 1983.Hepatic Adenoma and Focal Nodular Hyperplasia: Clinical Pathologic and Radiologic Features. gastro enenterology 84:994-1002.

Kssner, A, Thornhill, R, E 2010: A review of Neurologic MR, Imaging applications. Texture analysis:.,Am,J, Neuroradial .31, ,pp. 809-816 .

Classification, . IEEE Trans. Syst., Man, Cybern., Syst 3, , pp. 610-621.

Laws, K.I, 1980.Textured image segmentation. PhD thesis, University of Southern California.

Lerski, R.A., Straughan, K., Shad, L., Boyce, D., Bluml, S., Zuna.1993, I. Texture Analysis –An Approach toTissue Characterization. MR Image Magn. Reson. Imaging 11(8), pp. 873-887.

Mallat, S.G 1989 A theory for multi resolution signal decomposition: The wavelet representation. IEEE Trans. Pattern Anal. Mach. Intell. 11(7), pp. 674-693.

Mandelbrot, B block W. H. Freeman and Co, NY, 1982. The Fractal Geometry of Nature

Matt, A. Morgan et al, 2016.web site: [https://radiopedia.org/articles/ cystic hepatic metastases](https://radiopedia.org/articles/cystic-hepatic-metastases) .Visited on 17 1 2017 . at 6 :300 pm

Monfredi .S, Lepage. C, Hatem C, et al. 2006. Epidemiology and Management of Liver Metastases from Colorectal Cancer. Ann surg:244:254-259

Na Hwang, Ju Hwan Lee, Ga Young Kim ,Yuan Yuan Jiang ,and Sung Min Kim, Yoo,(2015).Classification of focal Liver lesions on ultrasound images by extracting hybrid textural features and neural network . Bio-Medical Materials and Engineering, 26S 1599- S1611.

Nihir n.Dalwadi, Prof D.N, khandhar,prof,kinita.h. wandra, July 2013. Automatic Boundary Detection and Generation of Region of Interest for Focal Liver Lesion Ultrasound Image Using Texture Analysis. International Journal of Advanced Research in Computer Engineering & Technology. (IJARCET). Volume 2, Issue 7.

Nimisha Manth, Jetendr Vermani, Vinod Komar , Navin Kaira, and khandelwal 2013. Application of texture features for classification of primary benign and malignant and primary malignant focal liver lesions. Image features, detections, and descriptions. Volume 630 of the Series Studies on Computational Intelligence. PP.385-409.

Owen Kang , and Dr Yuranga Weerakkody etal, 2017. Web site: [https://radiopedia.org/articles/ primary hepatic lymphoma](https://radiopedia.org/articles/primary-hepatic-lymphoma) Visited on 19/ 1/ 2017/ at 8:30 pm

Radswiki et al, 2017. web site:

[https://radiopedia.org/articles/biliary cyst adenoma](https://radiopedia.org/articles/biliary_cyst_adenoma). Visited on 17/1/2017,at 5:10 pm .

S.poonguzhali and ravindran2008. Automatic classification of focal lesions in ultrasound liver images using combined texture features. International technology journal, 7(1):205-209.

Saida 2015 Assesment of Liver Abscesses by using Ultrasound and Ultrasound guided drainage, Sudan University of science and technology, College of graduates studies.

Sakijan, (December 1988). Ultrasound finding of liver abscess, Med j.Malysia, vol 43. No 4.

Suleiman salih, Ahmed Elhaj. April 2014. Ultrasonography appearance of hepatic metastases from female breast cancer in patients in central Sudan. Journal of dental and medical sciences(IOSD-JDMS) .volume 13,issue 4 ver. VII.(), pp. 95,98

Suzan Standring ,PhD , DSc, FKc, 2008 .Grays Anatomy 40<sup>th</sup> Edition .  
The internal journal of gastroenterology, volume 5, number 2.

V.Ulagamuthalvi, D.Sridharan 2012, Automatic Identification of Ultrasound Liver Cancer Tumors Using Support Vector Machine. International Conference on Emerging Trends in Computer and Electronics Engineering.

V.Ulagamuthalvi and D.Sridhara, August 2012. Development of Diagnostic Classifier For Ultrasound Liver Lesion Images, international journal of computer applications (0975- 8887), volume 52-no 18 , pp.( 12-15).

Valerie C. Scanlon 2008 Essential of Anatomy and Physiology .

Vishwanath.T.Thimmaiah,2013. Evaluation of Focal Liver Lesions By Ultrasound as a Prime Imaging Modality, Scholars Journal Of Applied Medical Science {SJAMS}:1 (6): PP1041-1059.

Weszka, J.S., Dyer, C.R., Rosenfeld, A.1976: A Comparative Study of Texture Measures for Terrain Classification, IEEE Trans. Systems, Man, Cybernetics, 6,

Yuranga Wearakkody et al, 2017. Web site:  
site [https://radiopedia.org/articles/ biliary cyst adenocarcinomas](https://radiopedia.org/articles/biliary_cyst_adenocarcinomas). Visited on 17/1/2017 at 5 :30 pm.

Yuranga Wearakkody et al, 2016. Web site :  
[https://radiopedia.org/articles/ Amoebic hepatic abscess-1](https://radiopedia.org/articles/Amoebic_hepatic_abscess-1) visited on 17/1/2017 at 4 :20 pm

Zishan shekh and dryurangaweerakkodyetal2016. Web site:

<https://radiopedia.org/articles/polycystic-liver-disease-2016>. Visited on 17/1/2017/  
at 10 am

## APPENDICES

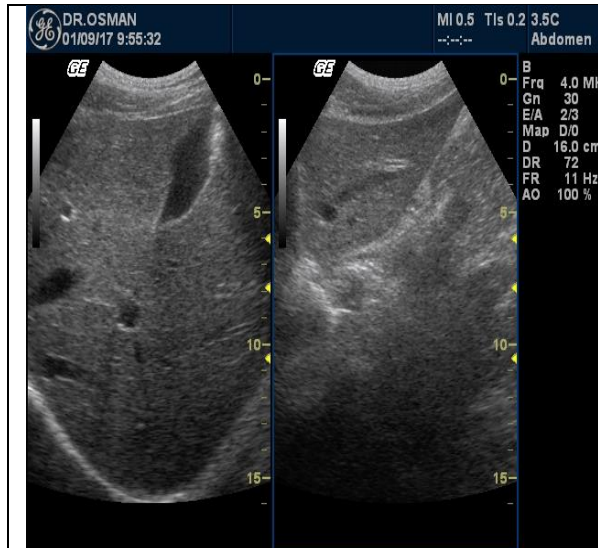


Fig- 1 showed a 54 years male normal liver size and texture

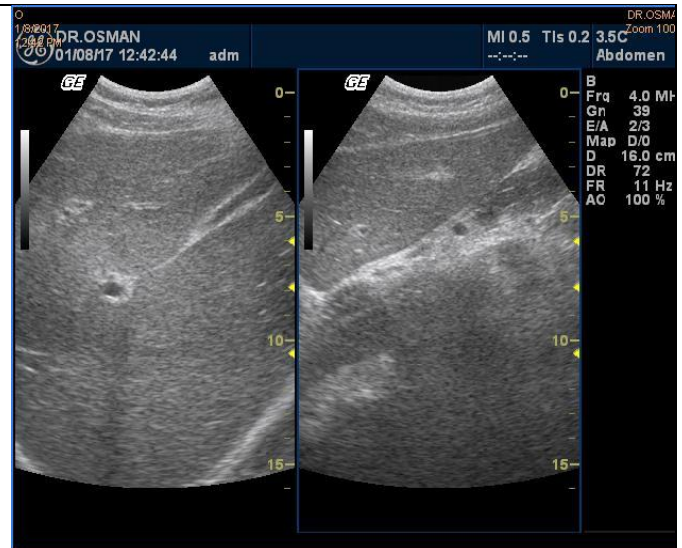


Fig -2 showed a 60 years male with normal liver size and texture

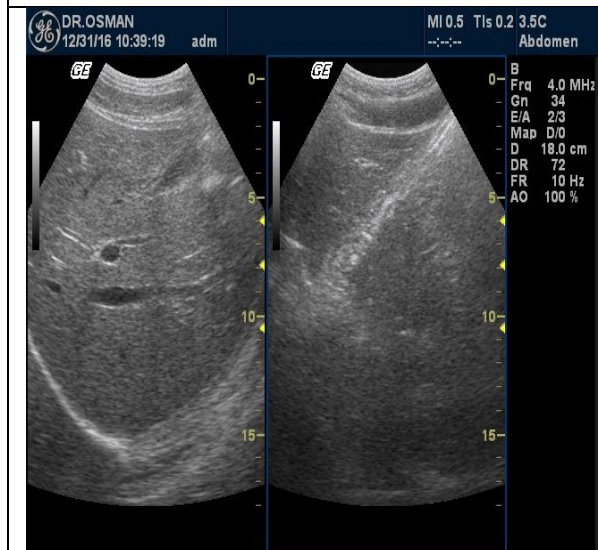


Fig- 3 showed a 40 years male with normal liver size and texture

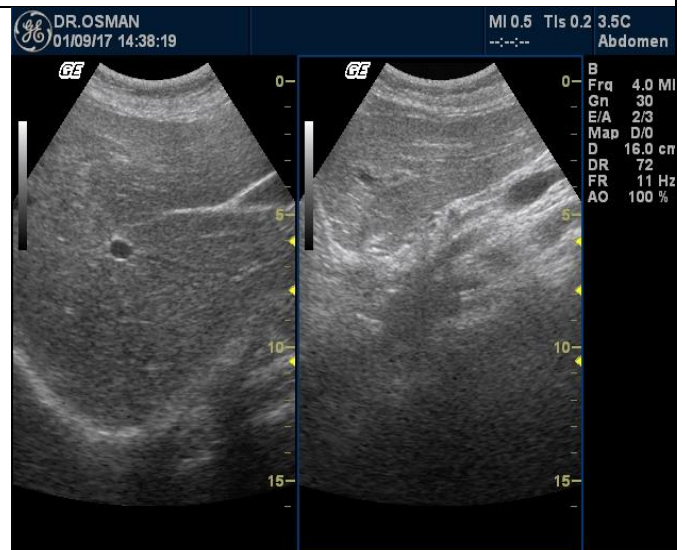


Fig -4 showed a 70 years male with normal liver size and texture

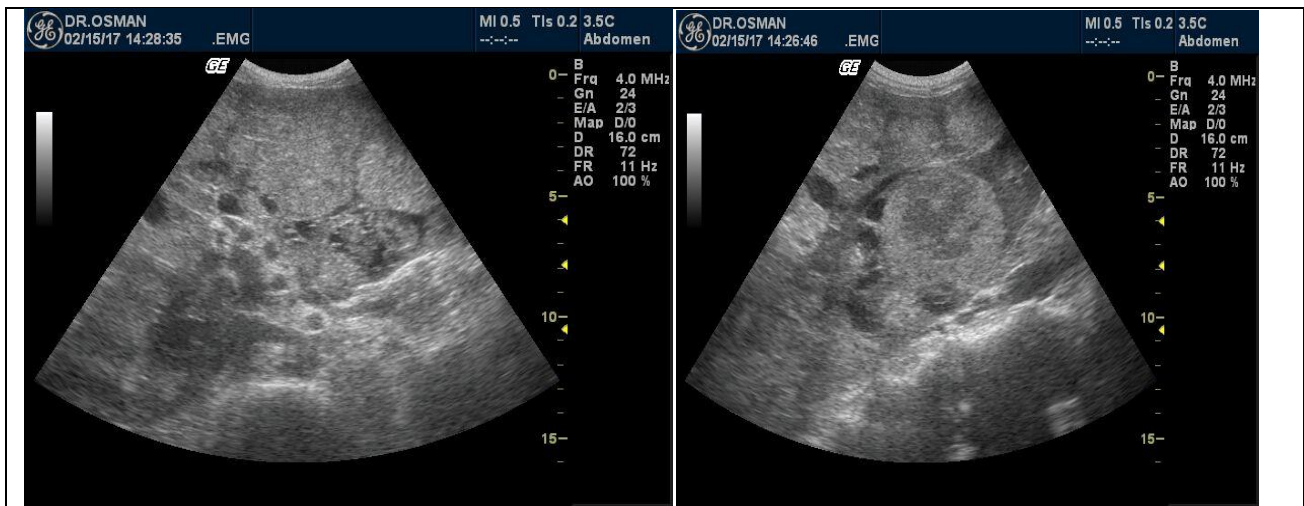


Fig-5 showed a 55 years female had enlarged liver with multiple hypo and hyper echoic rounded shape lesions (Metastases)

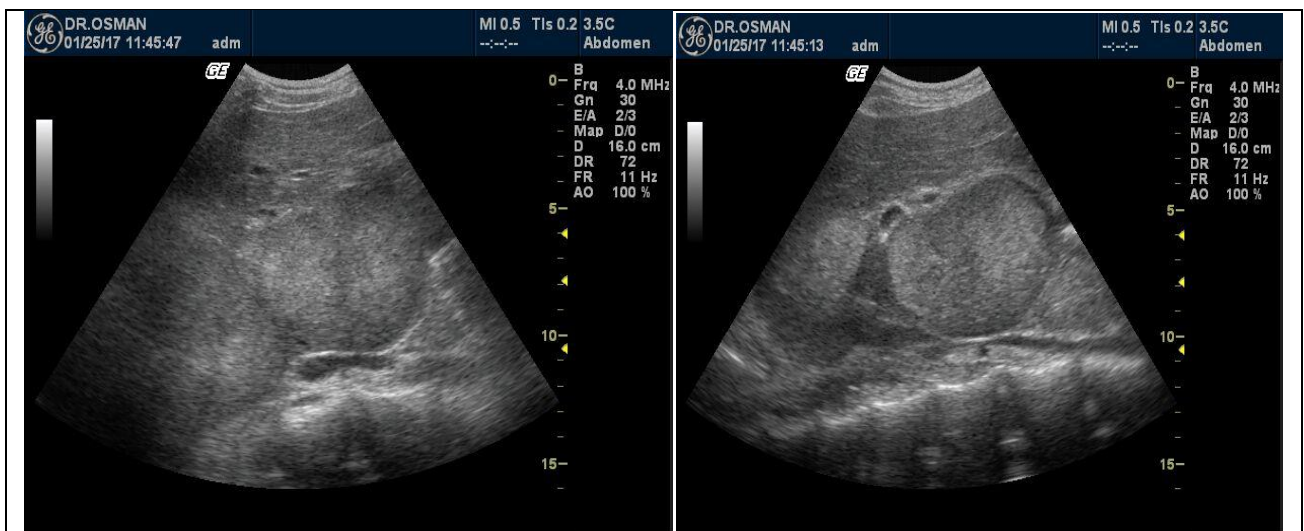


Fig-6 showed 52 years female had enlarged liver multiple hypo echoic lesions in both Rt& Lt lobe

(Metastases)





FIG-7 showed a 80 years female had enlarged liver with right multiple rounded hypo echoic lesion different sizes (Metastases)



Fig-8 showed a 62 years male had enlarged liver size and multiple hyper echoic lesions in both lobes (metastases)

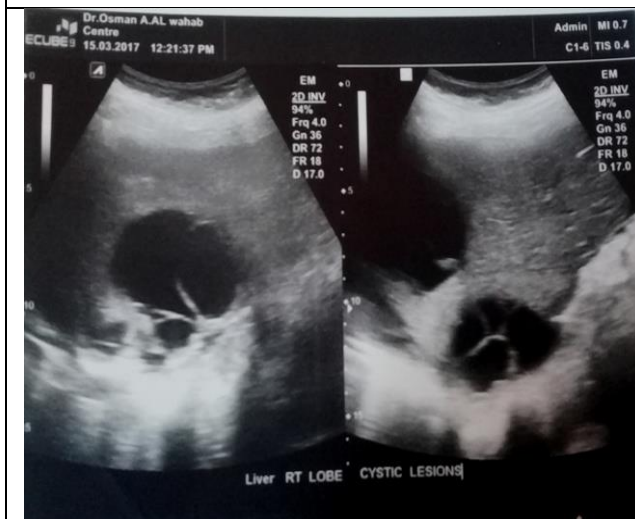


Fig-9 showed tow multiloculated cystic lesions in the right lobes posteriorly (Cystic metastases)



Fig-10 showed a 75 years female had multiple hyper echoic lesions with different sizes I n the right lobe (metastases)





Fig-11 showed 45years female , with enlarged liver with tow rounded un echoic lesions the big one in the right lobe ,small one in the left lobe with acoustic enhancement.(liver cyst)



Fig-12 showed a 60 years male had rounded un echoic lesion in the right lobe with acoustic enhancement.(liver cyst)



Fig-13 showed a 55years female , had liver with rounded lesion in the right lobe with acoustic enhancement.(liver cyst)



Fig -14 showed a 69 years female , had multiple rounded un echoic lesions in the left lobe with acoustic enhancement.(multiple liver cysts)

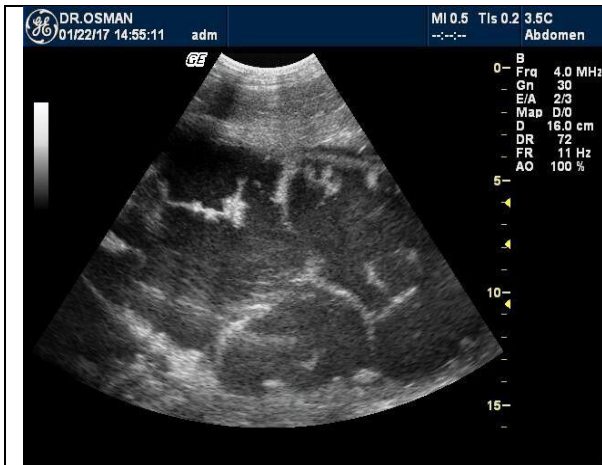


Fig -15 showed a 55 female had large thick wall cyst with septation and internal echoes. (hydated cyst)



Fig-16 showed a 67 years female had huge lobe septated lesion with wall calcification( Hydatid cyst)



Fig-17 showed a 12 years male had large rounded cystic lesions with solid component in both right and left liver lobes .( Hydatid cyst)



Fig-18 showed a 50 years male had right large solid lesion with multiple cystic areas within that. suggest hydated cyst

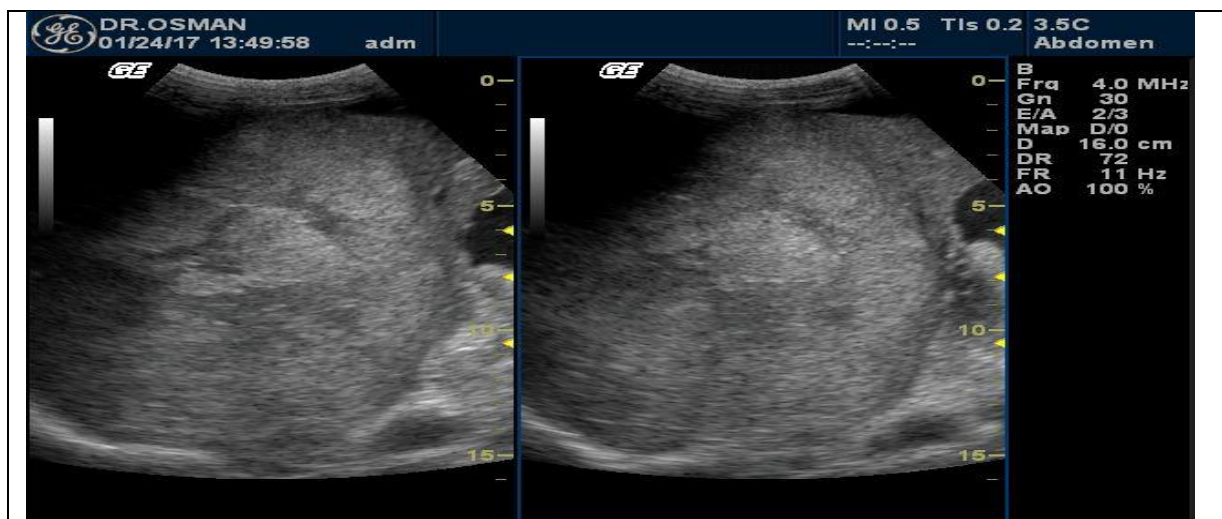


Fig-19 showed a 70 years old male had enlarged liver with coarse echo texture, with big rounded well defined hyper echoic with irregular outline and central necrotic changes.( HCC)

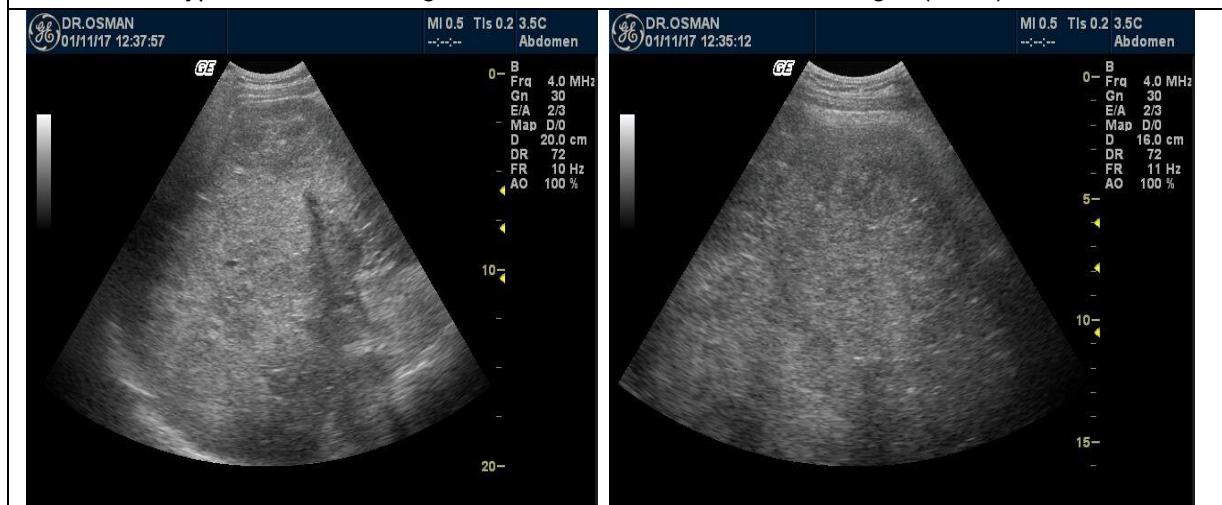


Fig-20 showed a 48 ears male had larged hyperechoic right lobe loulated mass (HCC)



Fig -21 showed a 70 years male had normal liver texture and size with large hypoechoic lesion with halo sign in the right lobe Hcc



Fig-22 showed the same patient



Fig -23 showed a 68 years female had small coarse liver texture with large heterogenous rounded well define lesion years male had small coarse texture liver (cirrhotic) with right lobe rounded hypoechoic lesion



Fig-24 showed a 62 years male had small coarse texture liver (cirrhotic) with right lobe rounded hypoechoic lesion



